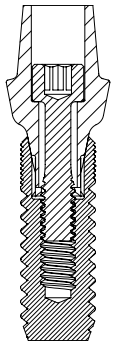

TUFTS UNIVERSITY
DEPARTMENT OF MECHANICAL ENGINEERING

EFFECT OF INSTALLATION PROTOCOL ON INITIAL PRELOAD LOSS IN DENTAL IMPLANT ABUTMENT SCREWS

A thesis submitted by

MICHAEL A. CASELLI
Tufts University
DENTSPLY Implants, Waltham, MA

In partial fulfillment of the requirements for the degree of

MASTER OF SCIENCE

in

MECHANICAL ENGINEERING

August 2013

Thesis Review Committee:

Thomas P. James, PhD
Associate Professor, Tufts University. Thesis Advisor

Anil Saigal, PhD
Professor, Tufts University. Committee Member

James G. Hannoosh, PhD
Vice President, ATLANTIS Development, DENSTPLY Implants. Outside Committee Member

Abstract

Restorative dentistry is turning increasingly to implant-supported restorations as a means to replace missing teeth. Nearly all implant-supported restorations involve at least one screwed joint. The purpose of the screw in these joints is to create a clamping force, called preload, between the joint members. If the preload in such a joint is degraded, the screwed joint can become more susceptible to failure. Often screwed joints will experience some initial loss of preload after they are first tightened. The purpose of this in-vitro study is to determine whether a dental implant abutment screw installation protocol that includes retightening of the screw; or tightening followed by loosening and retightening of the screw, can decrease the amount of initial preload loss. The study used 139 M1.6 titanium abutment screws of two different seating surface geometries in a simulated implant/abutment assembly that included a strain gauge for direct measurement of joint preload. Following tightening to 25 N-cm, preload was recorded for 2–12 hours. Preload loss and residual preload were evaluated at 2 hours. Without retightening, mean preload loss was 2.0% for the screw with the flat seating surface and 3.4% for the screw with the tapered seating surface. The simple retightening protocol produced the lowest mean preload loss, 0.8% for the flat screw, and 1.0% for the tapered screw. Without retightening, mean residual preload was 373 N for the flat screw 228 N for the tapered screw. Tightening, loosening and retightening produced the highest mean residual preload for the tapered screw (238 N). Neither of the retightening procedures had a statistically significant effect on mean residual preload for the flat screw ($p > .05$), though tightening, loosening and retightening cut the range of residual preload by more than

half compared to tightening alone. Scanning electron microscopy, white light interferometry, and profilometry were utilized to examine the contact surfaces after testing. Based on the results of this study, installation protocols involving retightening should be considered as a means to decrease relative preload loss, increase residual preload, and decrease variability in preload for dental implant abutment screws.

Acknowledgments

My first recognition must go to my wonderful fiancé for her support and for her expert statistical guidance. Sincere thanks to Dr. Jim Hannoosh for being such an outspoken advocate for me in my pursuit of advanced degrees. Thanks also to my very capable colleagues at ATLANTIS for their assistance, support, and understanding. Thanks to Amrit Sagar for the Zygo images, and Mike Mangaudis at Mikrotek Analytical for the SEM images. Finally and not least, thanks to Tom James and Anil Saigal for all their help on this project, and for putting such effort into their teaching. I've learned a lot from you two over the years.

Contents

List of Figures 7

List of Tables 9

1 Introduction 13

2 Research Objectives 13

2.1 Hypothesis 14

2.2 Secondary Objectives 14

3 Background 14

3.1 Components of a Typical Single-Tooth Implant-Supported Restoration 15

4 Problem Statement 17

5 Prior Research 18

5.1 Preload Loss 18

5.2 Installation Protocol 19

5.3 Unpredictable Preload 20

5.4 Variability of Applied Torque 23

6 Overview of Research Methods 25

7 Pilot Study 26

7.1 Implications for the main study 27

8 Main Study Materials and Apparatus 33

8.1 Apparatus 33

8.2 Abutment screws 35
8.3 Simulated Implant Threads and Simulated Abutment Counterbore 36
9 Main Study Methods 37
9.1 Experimental Design 37
9.2 Cleaning and Handling 38
9.3 Test Setup 39
9.4 Group T 42
9.5 Group TT 43
9.6 Group TLT 44
9.7 Statistical Methods 46
9.8 Wilcoxon Rank Sum Example Calculation 48
10 Roughness Measurement Methods 52
11 Scanning Electron Microscopy Methods 53
12 White Light Inferferometry Methods 54
13 Main Study Results 54
13.1 Initial Preload 55
13.2 Residual Preload 60
13.3 Relative Preload Loss 64
13.4 Absolute Preload Loss 66
14 Roughness Measurement Results 69
15 Scanning Electron Microscopy Results 71
16 White Light Interferometry Results 80
17 Discussion 84
17.1 Screw Stiffness 84
17.2 Tapered vs. Flat Screws 86
17.3 Magnitude of Relative Preload Loss 87

17.4 Effect of Installation Protocol on Relative Preload Loss 88
17.5 Effect of Installation Protocol on Residual Preload . . 89
17.6 Effect of Installation Protocol on Initial Preload 90
17.7 Roughness Measurement 91
17.8 SEM Images 91
17.9 Interferometry Images 93
18 Conclusions 94
19 Future Work 95

Works Cited **96**

Further Reading **99**

Appendices **106**
A Pilot Study Procedure 107
B Pilot Study Test Program 111
C List of Materials and Apparatus for Main Study 112
D Main Study Procedures 112
E Tabular Data: 2 Hours 118
F Tabular Data: 12 Hours 121
G Randomization Plan 123
H Randomization Plan for Roughness Measurement 128

List of Figures

1 Cutaway illustration showing a single-tooth, implant-supported restoration 16

2 Cross section drawing of abutment, abutment screw, and implant 17

3 Relative magnitude of the three reaction torques which oppose installation torque, typical 22

4 Abutment screws from main study, on 1 mm graduations . . . 26

5 Pilot study load vs. time 28

6 Test sensitivity vs. group size 29

7 Fraction of 12 hour load loss vs. time 30

8 Key dimensions of an abutment screw 31

9 Instron 55MT 33

10 Top view of custom load cell fixture 34

11 Cross section through assembled load cell fixture 34

12 Donut load cell, removed from fixture 35

13 Abutment screws from main study, on 1 mm graduations . . . 36

14 Threaded insert ST-009-M1.6 and hex insert ST-005-12 for tapered screw 37

15 Screws in cleaning cassettes 40

16 The Instron 55MT torsion test machine, ready for a test . . . 41

17 Close-up of the Instron 55MT torsion test machine, showing the abutment screw driver engaging the abutment screw 42
18 Two-sample univariate data corresponding to the null hypothesis 49
19 Two-sample univariate data corresponding to the alternate hypothesis 50
20 Roughness measurement apparatus 53
21 Location of roughness measurement sample length 53
22 Initial preload 56
23 Preload rise on second tightening, TT group 58
24 Residual preload after 120 min 61
25 Relative load loss after 2 hours 65
26 Absolute load loss after 2 hours 67
27 Ra (as measured) by protocol, flat screw 70
28 SEM images, unused screw head seating surface 72
29 SEM images, screw head seating surface, T protocol 73
30 SEM images, screw head seating surface, TT protocol 74
31 SEM images, screw head seating surface, TLT protocol 75
32 SEM images, counterbore seating surface, T protocol 76
33 SEM images, counterbore seating surface, TT protocol 77
34 SEM images, counterbore seating surface, TLT protocol 78
35 White light interferometry images, 5979 screw, T protocol . . 81
36 White light interferometry images, 5979 screw, TT protocol . 82
37 White light interferometry images, 5979 screw, TLT protocol . 83
38 Cross section of an implant-screw-abutment assembly showing critical abutment screw dimensions 108
39 Cross section of an implant-screw-abutment assembly showing critical abutment screw dimensions 114

List of Tables

1 Range of torque values produced by dentists using hand-held screwdrivers in a lab bench-top environment (From [6]) 24

2 Summary of pilot test results 27

3 Screw dimensions 36

4 Number of experimental trials in each experimental group . . 38

5 Example Wilcoxon rank sum data, null condition 50

6 Example Wilcoxon rank sum data, alternate (non-null) condition 51

7 Number of experimental trials in each experimental group . . 55

8 Mean initial preload 56

9 Pairwise Wilcoxon rank sum test p values: initial preload, tapered screw 57

10 Pairwise Wilcoxon rank sum test p values: initial preload, flat screw 59

11 Mean residual preload 60

12 Pairwise Wilcoxon rank sum test p values: residual preload, tapered screw 61

13 Pairwise Wilcoxon rank sum test p values: residual preload, flat screw 62

14 Pairwise F-test p values: residual preload, tapered screw . . . 63

15 Pairwise F-test p values: residual preload, flat screw 63

16 Mean relative preload loss 64
17 Pairwise Wilcoxon rank sum test p values: relative preload loss, tapered screw 66
18 Pairwise Wilcoxon rank sum test p values: relative preload loss, flat screw 66
19 Mean absolute preload loss 67
20 Pairwise Wilcoxon rank sum test p values: absolute preload loss, tapered screw 68
21 Pairwise Wilcoxon rank sum test p values: absolute preload loss, flat screw 69
22 Mean average roughness Ra (as measured, microns), flat screw 70
23 Pairwise Wilcoxon rank sum test p values: Average roughness (Ra), flat screw 71
24 Screw stiffness and relaxation, flat screws, pilot and main study 85
25 Screw dimensions 113
26 Instron Partner software test procedures 113
27 Raw data, observations after 2 hours, flat screw 118
27 Raw data, observations after 2 hours, flat screw 119
28 Raw data, observations after 2 hours, tapered screw 120
28 Raw data, observations after 2 hours, tapered screw 121
29 Raw data, observations after 12 hours, flat screw 122
30 Raw data, observations after 12 hours, tapered screw 122
30 Raw data, observations after 12 hours, tapered screw 123
31 Randomization plan for 2-hour observation period 123
31 Randomization plan for 2-hour observation period 124
31 Randomization plan for 2-hour observation period 125
31 Randomization plan for 2-hour observation period 126

32 Randomization plan for 12-hour observation period 127
33 Randomization Plan for Roughness Evaluation 128
33 Randomization Plan for Roughness Evaluation 129

1 Introduction

Stable abutment screw preload is a major factor in the longevity of an implant-supported dental prosthesis. One study found that within 5 years of placing a single crown implant supported restoration, screw loosening was reported for 12.7% of cases, and screw fracture was reported in 0.35% of cases, making screw loosening the "most common technical complication" for this type of case [9].

Bolted joints begin to lose preload the instant the wrench is removed from the bolt upon tightening, through a mechanism known as embedment relaxation [2]. Various abutment screw installation protocols have been proposed by researchers and implant manufacturers in an attempt to reduce the magnitude of initial preload loss [3], [15], [17].

This in-vitro study examines the effectiveness of three different abutment screw installation protocols in terms of reducing initial abutment screw preload loss in an implant-abutment assembly that is not subject to external loading. Two abutment screw configurations were tested: a screw with a tapered seating surface and cut threads, and a flat-headed screw with rolled threads.

2 Research Objectives

The objective of this research is to examine the effects of three different abutment screw installation protocols in terms of reducing initial abutment screw preload loss, and to seek an understanding of why the method of tightening and the contact geometry of the screw appear to affect the rate of preload degradation.

This research focuses on the degradation of preload intrinsic to the joint itself, and excludes the effect of external, functional loading (i.e. chewing).

2.1 Hypothesis

The sequence in which torque is applied to a dental implant abutment screw, such as to tighten and retighten, or to tighten followed by loosening and retightening, has a significant effect on the immediate degradation of screw preload prior to the application of external loading.

2.2 Secondary Objectives

The study is also intended to provide insight into the following questions:

- How much initial preload loss can be expected for new abutment screws in new implants?
- What is the effect of a tapered screw seating surface on initial preload loss?
- What is the effect of the various installation protocols on the initial preload for new abutment screws in new implants?
- Do the various proposed "re-torquing" protocols reduce variation in joint preload?
- Can scanning electron microscopy or profilometry detect a change in the roughness of the mating surfaces of the abutment screw that would help to explain any observed difference in initial preload or initial preload loss?

3 Background

Dental implants are becoming a more common method of replacing missing teeth for partially or fully edentulous patients. Compared with alternate meth-

ods such as conventional crowns, bridges, fixed partial dentures, and removable dentures, restorations based on dental implants can last longer [16], provide increased functionality, and often require less modification of surrounding healthy teeth [14]. Studies have shown that dental implant treatment is a cost-effective treatment method compared to fixed partial dentures or other "traditional treatments" for partial edentulism [19]. Due to increased awareness of the benefits of implant-based restorations, and the aging of the baby-boomer generation, the dental implant market in North America has been projected to grow at approximately 9% per year over the period 2010–2014, with 2.1 million implant procedures forecast for 2014 [12].

An implant-supported replacement for a single tooth can often involve five or more individual components, held together by methods including screws and adhesive bonding. Nearly all implant-supported restorations, whether single-tooth or multi-unit, involve at least one mechanical screwed joint. Commonly, an abutment of some type is retained to the dental implant using a screw, and the final restorative components are secured to the abutment either by adhesive bonding [20], snap-retentive features [11], or yet another screwed joint [20].

3.1 Components of a Typical Single-Tooth Implant-Supported Restoration

The *dental implant* is essentially a bone screw with some sort of provision for attaching restorative components (these attachment features are often referred to as the *implant interface*). The job of the implant is to provide an anchor point for the restoration. The implant is surgically placed into the jaw bone, such that its coronal end[1] is about even with the level of the crest of the

[1]The coronal end of the implant is the end facing into the mouth, as opposed to the apical end, which faces into the jaw bone.

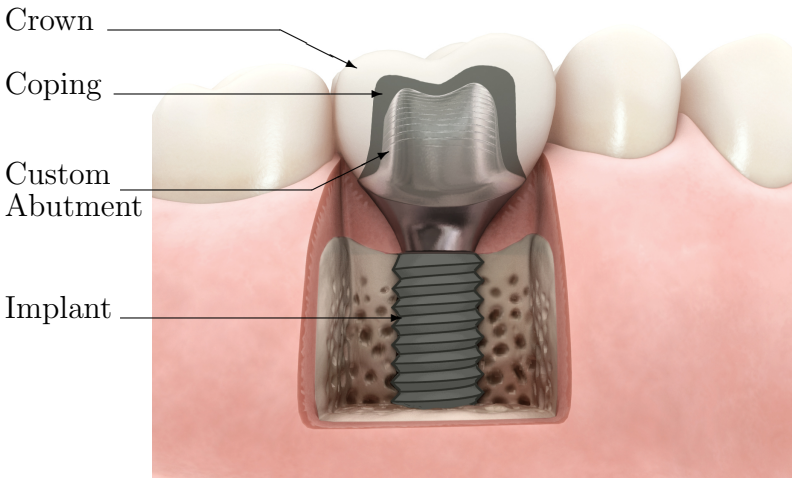

Figure 1: Cutaway illustration showing a single-tooth, implant-supported restoration. Not shown: abutment screw, coping cement. Image courtesy DENTSPLY Implants.

bone (see Figure 1). One common class of implant connects to restorative components using a socket formed inside the coronal end of the implant, with a set of female threads apical of the socket (see Figure 2).

In the case of a single-tooth restoration, the next component in the restorative stack is usually an *abutment*, which engages the implant interface and is secured with an *abutment screw*. The job of the abutment is to extend the structure of the implant system and to provide support for the final restoration. Abutments are typically made of metals such as gold alloys and titanium alloys, or of ceramic materials such as zirconia. Restorations can be either cement-retained or screw-retained to the abutment.

The *crown* is the visible part of the restoration, typically made of porcelain or other ceramics. In the case of cement-retained restorations, the porcelain that makes up the visible part of the crown is glazed onto the surface of a *coping*, typically made of metals such as gold alloys and titanium alloys, or of ceramic materials such as zirconia. The coping and crown, now one unit, are then cemented to the abutment as the last step in the restorative process.

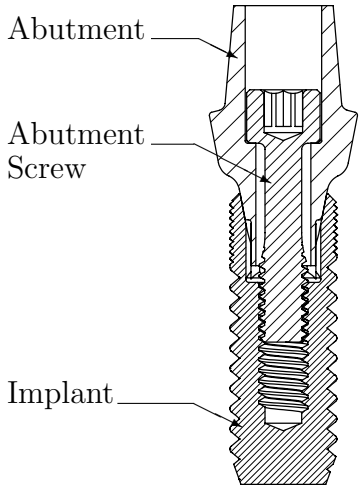

Figure 2: Cross section drawing of abutment, abutment screw, and implant

4 Problem Statement

Bolted joints undergo a loss of preload beginning the instant after they are tightened [2, p. 196]. This loss of preload can leave the joint less able to perform its intended function, and may leave the joint more susceptible to failure.

This immediate loss of preload is due to a phenomenon that has been called short-term relaxation [2, p. 190]. Much of this short-term relaxation is due to highly localized yielding at the contact surfaces of the joint, and can be termed embedment relaxation [2, p. 190]. There are many factors that influence relaxation, and they can be difficult to predict. As a result, experimental methods are required to determine how much relaxation to expect for a given application, and even then, the part-to-part variability can be large [2, p. 196].

Functional loads (in this case, chewing loads) may serve to exacerbate the embedment effect, contributing to further preload loss. Lower residual preload can lead to increased fatigue effects for a joint subject to cyclical external loading, by increasing the amplitude of the load excursion seen by the bolt [2, p. 583]. This leaves the joint more susceptible to fatigue failure.

Loosened or broken abutment screws require a return visit to the dentist, and it is likely that the crown or bridge and the abutment would have to be destroyed to retrieve the loose or broken screw. A loose or broken screw also creates certain clinical risks, such as the potential for the patient to inhale or swallow an unsecured restoration, or the potential for damage to the gingiva (gum tissue) stemming from movement of the restoration.

A systematic review of 26 studies by Jung, Pjetursson, Glauser, *et al.* found that within 5 years of placing a single crown implant supported restoration, screw loosening was reported for 12.7% of cases, making screw loosening the "most common technical complication" for this type of case. The study also found that the cumulative incidence of screw fracture after 5 years in service was 0.35% [9].

Various screw installation protocols have been suggested by researchers or recommended by implant manufacturers. Some of these protocols are in direct conflict with each other [3], [15], [17].

5 Prior Research

Many papers have been published on dental implants and screws used in implant-supported restorations. A number of key research areas are relevant to the current study.

5.1 Preload Loss

Cantwell and Hobkirk conducted a study examining the embedment relaxation that takes place in gold alloy prosthetic retaining screws (small screws used to attach a final restoration, such as an implant supported framework, to a standard abutment). Their study found a mean preload loss of 24.9% after

15 hours, with 40.2% of this loss occurring within 10 seconds of tightening [5].

The findings of Cantwell and Hobkirk demonstrate that embedment relaxation results in a significant amount of preload loss for screws used in implant-supported prostheses. The current study aims to determine which, if any, of the proposed installation protocols can reduce the magnitude of this preload loss.

5.2 Installation Protocol

A number of studies have been conducted looking at the effects of various installation protocols. Suggestions made by some researchers are in direct conflict with the findings of other researchers [4], [17].

Tzenakis, Nagy, Fournelle, *et al.* recommended the use of the final gold prosthetic screw at the try-in appointment, and the subsequent re-use of that screw at the final placement, as the increased preload and reduced settling effects could decrease the need for frequent re-torquing of the final restoration [17].

Byrne, Jacobs, O'Connell, *et al.* conducted a study of the preload from repeated torquing of abutment screws made of three different materials, and found that all screw types showed some decrease in preload with repeated tightening [4]. While the authors stopped short of making recommendations for clinical installation protocols, their findings are in conflict with Tzenakis, Nagy, Fournelle, *et al.*, which casts some doubt on the protocol suggested by Tzenakis, Nagy, Fournelle, *et al.*

An in-vitro study by Siamos and Winkler found that re-torquing abutment screws after 10 minutes reduced the percentage difference between installation torque and removal torque, and suggested that this protocol could reduce screw loosening [15].

Al Rafee, Nagy, and Fournelle performed an in-vitro study looking at the effect of repeated torque applications to gold prosthetic screws on the ultimate tensile strength of the gold prosthetic screw. They found that after 20 torque application cycles, no reduction in ultimate tensile strength was evident. Furthermore, they found that whether the torque application cycles were performed in a dry or in a saliva-lubricated condition had no impact on the ultimate tensile strength [1].

The lack of agreement in this body of prior research highlights a need for further research on the effects of various installation protocols. The apparatus and methods of the current study should produce more repeatable results than Tzenakis, Nagy, Fournelle, *et al.* and Byrne, Jacobs, O'Connell, *et al.*, and the results of the current study should provide some support for one of the two contradictory studies.

While the prior work mentioned here has examined the effects of installation protocol on *instantaneous* or *initial preload*, no research has been found comparing the *initial preload loss* of screws tightened using various protocol, which is arguably a more functionally relevant quantity. The current study aims to address this question.

5.3 Unpredictable Preload

When torque is applied to a screw or bolt, the input torque is balanced by three reaction torques, as shown in the following equation (from [2]):

$$T_{in} = F_P \left(\frac{P}{2\pi} + \frac{\mu_t r_t}{\cos \beta} + \mu_n r_n \right) \tag{5.1}$$

where T_{in} is the applied torque, F_P is the preload in the joint, P is the pitch of the threads, μ_t is the coefficient of friction at the threads, r_t is the effective

radius of contact of the threads, β is the half-angle of the threads (30°for ISO and UN threads), μ_n is the coefficient of friction at the screw head, and r_n is the effective radius of contact of the screw head.

The first term in Equation 5.1, $F_P \frac{P}{2\pi}$, is produced by the inclined plane of the threads, which causes the fastener to stretch. This is the component that produces the preload in the joint. The second term, $F_P \frac{\mu_t r_t}{\cos \beta}$, is the reaction torque caused by friction at the screw threads. The final term, $F_P \mu_n r_n$, is the reaction torque caused by friction under the screw head.

Bickford states that if one substitutes typical fastener dimensions and friction coefficients into the above equation, one finds that approximately 50% of the input torque goes to overcoming friction under the screw head (or between the face of the nut and the joint members, in the case of a bolted joint), and 40% of the input torque goes to overcoming friction at the screw threads. This leaves only 10% of the input torque remaining to stretch the fastener and generate the preload in the joint (Figure 3) [2].

Bickford goes on to lay out an illustrative thought experiment: suppose the friction coefficient at the screw head increases by a mere 10% (such a change could easily arise from variations in lubrication or surface condition), the fraction of input torque that goes to overcoming friction at the screw head then increases from 50% to 55%. This extra 5% of input torque cannot come from the friction at the screw threads, as nothing has changed there, it must instead come from the portion of the input torque that would otherwise have gone to stretching the fastener and creating preload. Thus the bolt stretch component has now been reduced from 10% to 5%—a 10% increase in friction at the screw head has resulted in a 50% decrease in preload. Bickford calls this a "leverage effect," which can give rise to large variation in preload [2].

Guda, Ross, Lang, *et al.* conducted a probabilistic analysis of the preload

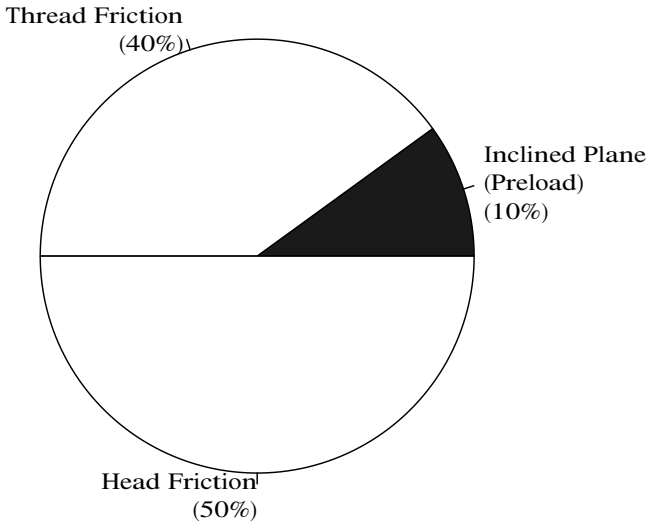

Figure 3: Relative magnitude of the three reaction torques which oppose installation torque, typical. Redrawn from [2].

generated in an abutment screw using Monte Carlo and similar methods [7]. For the specific system under examination, in a lubricated environment, the authors found the distribution of the preload generated to be a normal distribution with a mean of 617 N, and standard deviation of 92 N. With this distribution, one could reasonably expect the preload for any given screw to fall anywhere between 400 N and 800 N. Such a wide spread in the resultant preload is likely to lead to variations in the functional performance of the system.

A secondary objective of the current study is to determine whether installation protocol has an effect on the variability of the preload generated in the implant-abutment joint. An installation protocol that reduces variation in preload may be desirable to achieve more consistent performance from the implant-screw-abutment system.

5.4 Variability of Applied Torque

Much research has focused on the ability of dentists to tighten abutment screws and prosthetic retaining screws to a specified torque level. Some researchers have stated that it is common practice to tighten these screws by hand without the aid of a torque-indicating driver. The variability in applied torque that results when dentists tighten screws without the use of a torque-indicating driver is many times greater than what is achievable with the aid of a torque-indicating driver [6], [10], [18].

Kanawati, Richards, Becker, *et al.* conducted a very basic study that they claimed provided a method that clinicians could use to "calibrate their ability" to torque components by hand (i.e. without the use of a torque wrench). They measured the torque required to remove a healing abutment that had been installed using finger drivers. While the study may be somewhat flawed

Table 1: Range of torque values produced by dentists using hand-held screwdrivers in a lab bench-top environment (From [6])

Target (N-cm)	Min. (N-cm)	Max. (N-cm)
10	0.7	18.1
20	1.4	33.7
32	8.2	36.2

in its methods and conclusions[2], it gives some idea of the type of variability in installation torque that can result if clinicians are installing screws using finger drivers rather than torque wrenches. Across 50 subjects, they found that the torque required to remove a healing abutment installed using finger drivers varied from a minimum of 11 N-cm to a maximum of 38 N-cm, with a mean of 24 N-cm and a standard deviation of 6.2 N-cm [10].

Goheen, Vermilyea, Vossoughi, *et al.* conducted a study of 5 oral and maxillofacial surgeons and 11 prosthodontists to see how accurately they could torque dental implant components using only hand-held screwdrivers. This study did not make use of a typodont or simulated patient, so the ergonomics of this study are quite different from the clinical environment. They asked these dentists to torque various components to 10, 20, and 32 N-cm, and measured the resulting torque using a digital torque sensor. A summary of the range of the results is in Table 1. The coefficient of variation ranged from 21–56% for the various groups in this study [6]. The wide range of torque values obtained in this study makes clear that torque control devices should be used to tighten implant components.

Goheen, Vermilyea, Vossoughi, *et al.* also examined the accuracy of various torque control devices on the market at the time of the study (1994), and found that all the manual (i.e. non-electronically driven) torque drivers did

[2]While Kanawati, Richards, Becker, *et al.* states that a pilot study was conducted showing that the removal torque required for these components was "the exact level" used to install the components, their measurement system was not very precise, and in general, removal torque and installation torque are not equal.

a good job of accurately and repeatably delivering the target torque [6]. A study conducted by Vallee, Conrad, Basu, *et al.* also demonstrates that the torque control devices available in the dental market are capable of delivering reasonably accurate and repeatable torque [18].

The findings presented here demonstrate that the variation in applied torque can be very high when dentists do not utilize torque control devices to install abutment screws or prosthetic screws. They also demonstrate that the torque control devices available are capable of delivering highly accurate and repeatable results. These studies therefore form the basis for examining installation protocols based on the use of torque control devices. Perhaps if a simple installation protocol using torque control devices can be shown to significantly reduce the loss of preload in abutment screws, more dentists will be persuaded to use torque control devices regularly in their practice.

6 Overview of Research Methods

All testing was conducted in-vitro.

A pilot study on preload loss was conducted to form the basis of a statistical power analysis for the main study. In the pilot study, five (5) M1.6 titanium abutment screws were torqued to 25 N-cm using an Instron torsion test machine and left to sit for 12 hours while the preload in the joint was recorded using a strain gauge.

The main study utilized the same Instron torsion test equipment to subject titanium abutment screws of two different designs (one with a flat seating surface, one with a tapered seating surface, see Figure 4) to three different installation protocols, yielding a total of six experimental groups. Within each experimental group, 23–24 experimental trials were conducted, using a new

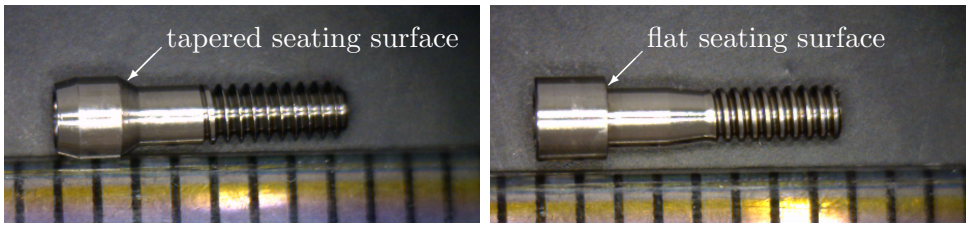

(a) Abutment screw 5764 "tapered screw"

(b) Abutment screw 5979 "flat screw"

Figure 4: Abutment screws from main study, on 1 mm graduations

screw, simulated abutment, and simulated implant for each trial ($n = 139$). Peak installation torque was 25 N-cm in all cases. Preload in the joint was recorded for either 2 hours or 12 hours after torque application, based on a pre-determined, block-randomized test plan.

Following the main study, a subset of the abutment screws and simulated abutment counterbores from the main study were subjected to surface characterization using scanning electron microscopy (SEM), white light interferometry, or profilometry, in an attempt to observe the effect that the various installation protocols had upon the surface finish of the underhead of the screw and the counterbore of the simulated abutment.

All data analysis was performed using R [13].

7 Pilot Study

A pilot study was undertaken in order to validate the test procedures, and to determine the observation time period and sample size necessary to achieve statistical significance in the main study.

Five (5) M1.6 abutment screws with a flat seating surface (article number 5346, DENTSPLY Implants, Waltham, MA, USA) were torqued to 25 N-cm and left to sit for 12 hours while the preload in the joint was recorded at a rate of 10 Hz.

Preload loss is defined here as the difference between the preload at a given time and the peak preload generated during tightening. The preload loss at 12 hours as a percentage of peak preload was 1.3–3.2% for the five screws studied, with a mean of 2.4%, and a standard deviation of 0.8% (Table 2).

Table 2: Summary of pilot test results, load loss and percent load loss over 12 hours, flat headed screw

Screw Number	Max Torque (N-cm)	Max Load (N)	Min Load (N)	Load Loss (N)	Pct. Load Loss
1	25.3	323	317	6	1.7%
2	25.2	308	299	9	3.0%
3	25.3	305	295	10	3.2%
4	25.3	304	296	8	2.6%
5	25.2	324	320	4	1.3%

The loss of preload is roughly linear over the 12 hour observation period when plotted on a log time scale (Figure 5). The jog in the load vs. time curves around 0.01 min corresponds to the time when the applied torque was being reduced to zero by the Instron 55MT.

7.1 Implications for the main study

A survey of the existing literature showed a preload loss on the order of 10–30%. The preload loss observed in the pilot study was well below this range.

The low mean preload loss combined with the high variability of preload loss dictated that a large number of replicates would be required to achieve reasonable statistical power.

An initial goal was to be able to detect a 20% difference in mean preload loss between experimental groups. A power analysis based on the results of this pilot study found that to have an 80% chance of detecting a 20% difference in mean percent preload loss, there would need to be more than 50 samples

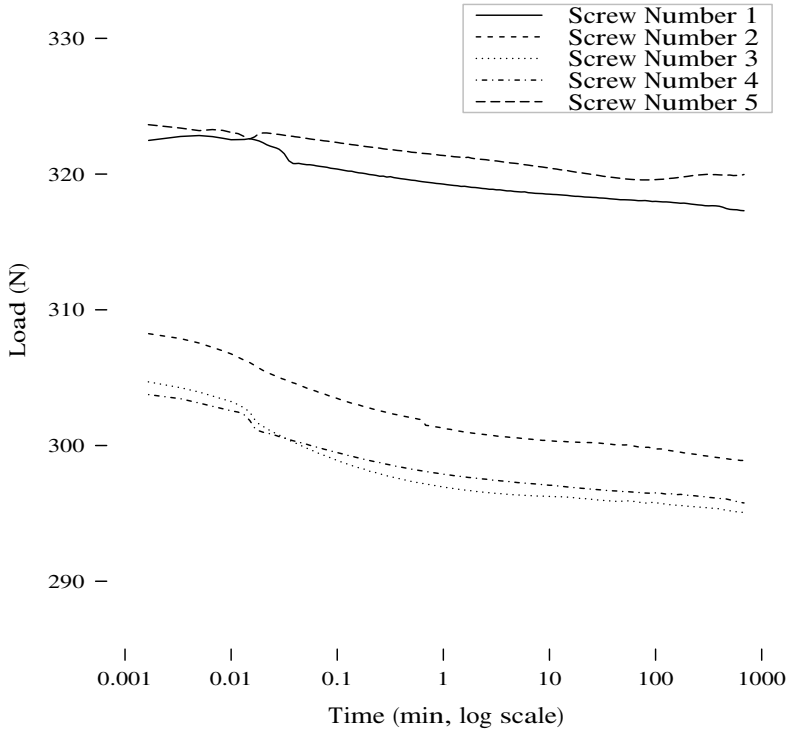

Figure 5: Pilot study load vs. time

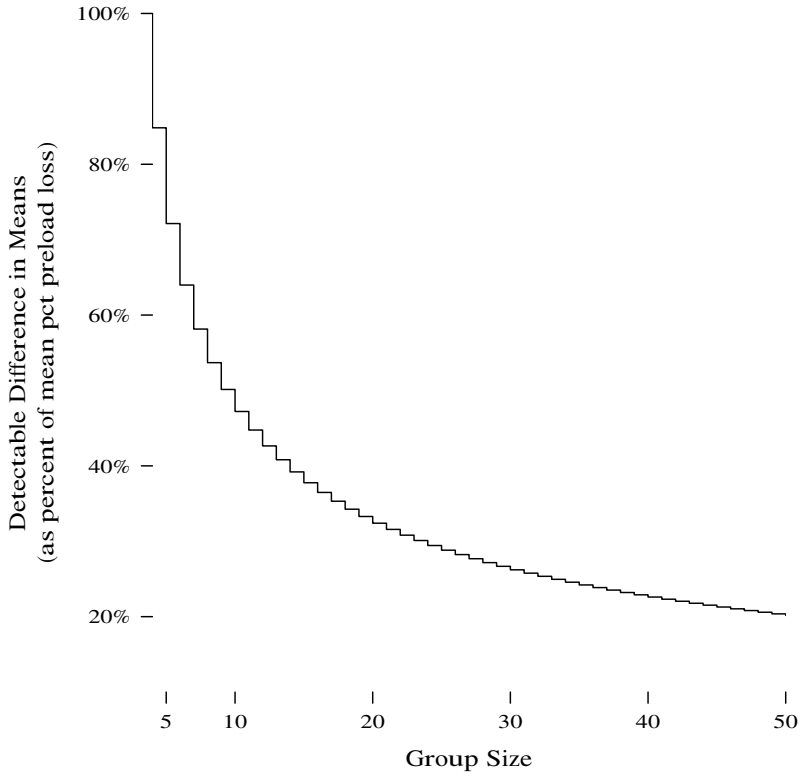

Figure 6: Test sensitivity vs. group size ($\alpha = 0.05$, $\beta = 0.2$)

per experimental group (Figure 6). With an experimental design containing six groups (3 protocols $\times$ 2 screw geometries), 50 samples per group makes a total of 300 experimental trials, which would not be feasible to observe for 12 hours each within the constraints of this study.

A revised goal was to explore what would be possible with a more moderate group size (20–30 experimental trials per group) and make adjustments to the materials and methods where practical in an attempt to increase the observed effect size (i.e. the difference in mean preload loss between groups), decrease the experimental variance, and reduce the time required to conduct the series of experimental trials. The purpose of these efforts was to maintain statistical power while reducing the required investment of time and effort to a level consistent with the resources available for the study.

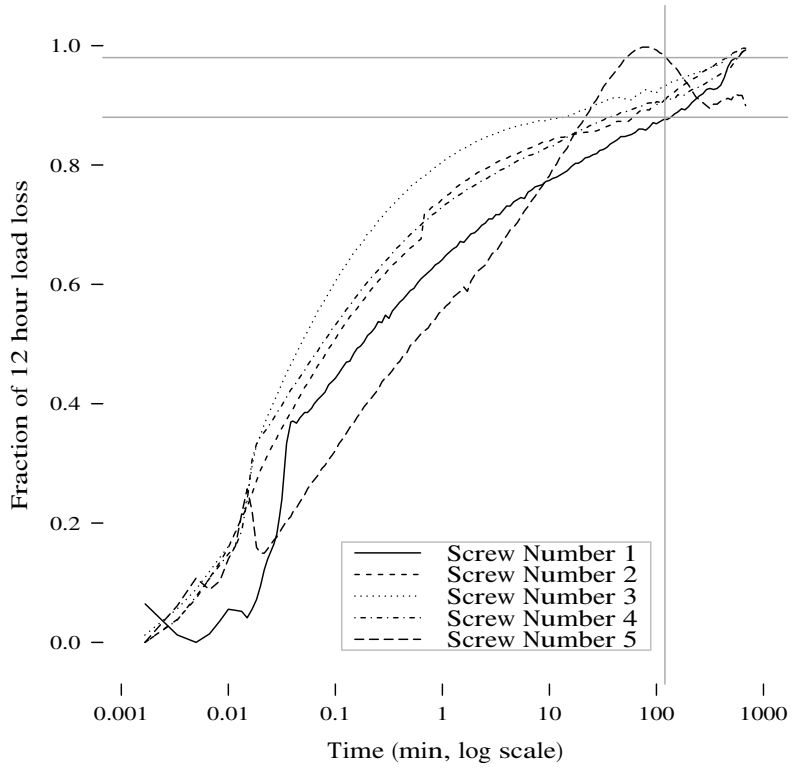

Figure 7: Fraction of 12 hour load loss vs. time (reference lines showing the range of observed values at 2 hour)

Attempts to reduce the time required to conduct the study focused on the observation period for each experimental trial. For the five tests conducted during the pilot study, a 2 hour observation period yielded between 88% and 98% of the total preload loss observed in 12 hours (Figure 7), a clear case of diminishing returns beyond an observation time of 2 hours. It was therefore decided to observe the majority of screws in the study for 2 hours, with a smaller number of screws being observed for 12 hours. A 2 hour observation period makes it feasible to include a larger number of samples in the study, improving statistical power. Observing a smaller number of screws for a full 12 hours provides a longer-term picture of the shape of the preload loss over time.

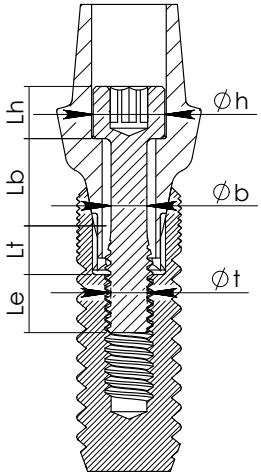

Figure 8: Key dimensions of an abutment screw

The power analysis based on the results of the pilot study showed that while requiring a statistical power of 80% ($\beta = 0.2$), a group size of 20 only allows one to differentiate between groups with at least a 32% difference in means (Figure 6). Concerned that it may not be reasonable to expect every group-to-group difference to be greater than 30% using the materials and methods of the pilot study, some adjustments were made to attempt to increase the effect size and decrease the variance.

One such change intended to improve the statistical power was to use shorter (and therefore stiffer) screws, in an attempt to create a larger drop in preload, which would be more readily observable using the load cell of the experimental apparatus.

The stiffness of a screw is proportional to its cross-sectional area, and inversely proportional to its length (Equation 7.1, Figure 8).

$$K = \frac{F_P}{\Delta L} = E\left(\frac{A_b}{L_b + L_h/2} + \frac{A_t}{L_t + L_e/2}\right) \tag{7.1}$$

The particular screw geometry used in the pilot study was relatively long and thin, making for a low stiffness screw.

The mechanism that is believed to be driving the preload loss in this study is embedment relaxation, where surface asperities at the contact areas of the joint are crushed, leading to a decrease in the elongation of the screw, which results in a loss of preload.

The elongation of the screw can be estimated based on geometry, material properties and load. By simply rearranging Equation 7.1, an expression for this elongation can be generated:

$$\Delta_L = \frac{F_P}{E}\left(\frac{L_b + L_h/2}{A_b} + \frac{L_t + L_e/2}{A_t}\right) \tag{7.2}$$

In a screw with low stiffness, such as the long screws used in the pilot study, a given decrease in elongation results in a small drop in preload; in a screw with higher stiffness, the same decrease in elongation results in a larger drop in preload.

This relationship was seen as a possible way to increase the statistical power of the study by increasing the effect size (i.e. increasing the drop in preload). With this in mind, the two screw types selected for the main study were considerably shorter, and therefore stiffer than the screws used in the pilot study.

In a further attempt to increase the statistical power, an effort was made to seek out and mitigate potential sources of experimental variance. It is likely that the cleanliness and surface condition of the contact areas of the parts plays a role in the tightening and settling behavior of the joint, therefore, a cleaning and handling procedure for the screws, threaded inserts, and hex inserts was incorporated in the main study in an attempt to control this effect.

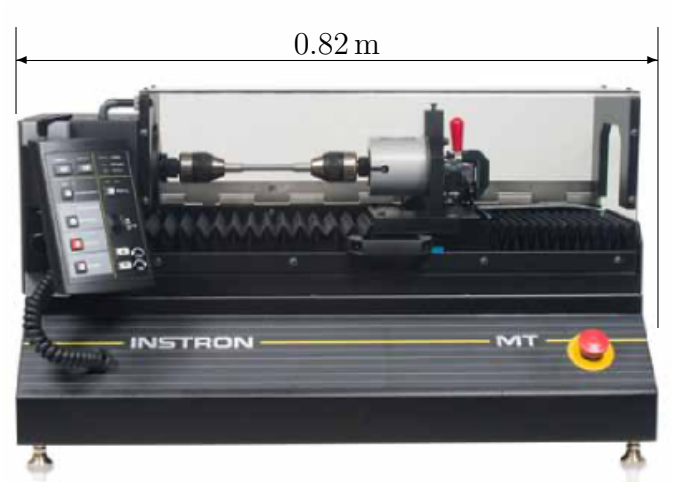

Figure 9: Instron 55MT (photograph from Instron product brochure)

8 Main Study Materials and Apparatus

8.1 Apparatus

The system is based on an Instron 55MT torsion testing machine (Instron, Norwood, MA, USA), shown in Figure 9. This Instron machine has a rotary encoder on the power head, and a torsion load cell on the tailstock.

The power head of the 55MT is capable of delivering a maximum torque of 2,200 N-cm, and the rotational resolution of the power head is 0.168 arc-min (0.0028°). For this application, the machine is fitted with a 225 N-cm capacity torque cell.

The power head can be operated under either rotation rate control or torque rate control. The tailstock can be allowed to slide freely in the axial direction on a low friction linear slide, and can be loaded either in tension or compression using a hanging weight of up to 220 N (50 lb). For this application, the tailstock is allowed to slide freely, and a nominal weight of approximately 5 N (1 lb) is used to provide axial compression to keep the screw driver engaged in the screw head.

The author designed a compressive load cell fixture that makes use of a

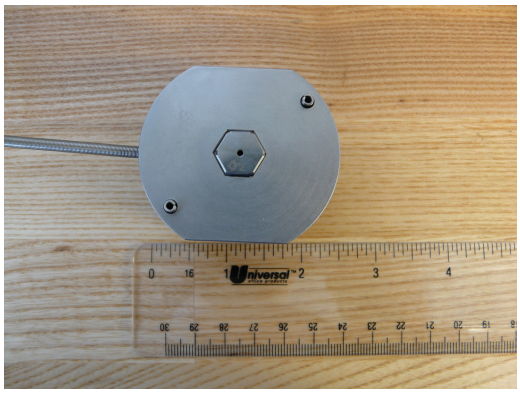

Figure 10: Top view of custom load cell fixture. The hex-shaped component on top is a simulated abutment counterbore surface

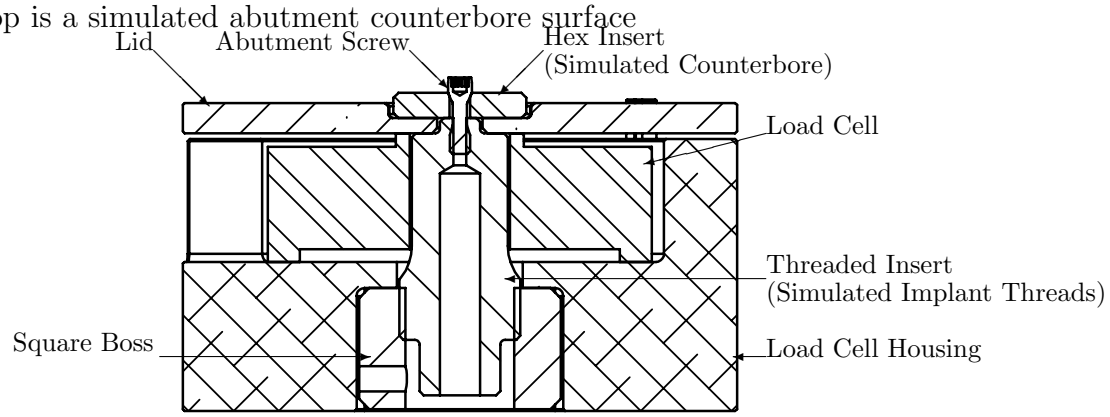

Figure 11: Cross section through assembled load cell fixture

3/8 inch ID donut load cell with a 1.1 kN (250 lb) capacity (Model D: BL913CN S, Honeywell Sensing and Control, Golden Valley, MN, USA) to measure the clamping force generated in a simulated implant/abutment joint (Figures 10, 12, 11). The output from this load cell is also fed into the Instron data acquisition hardware, so the the system is capable of recording torque, angle and preload simultaneously.

All systems and sensors are professionally calibrated and certified on an annual basis.

The author has not found any reference to such a capable and sophisticated system in any of the published literature on implant abutment screws or prosthetic retaining screws. The high quality of the sensors and the ability to control the rate at which the screw is tightened should greatly reduce the

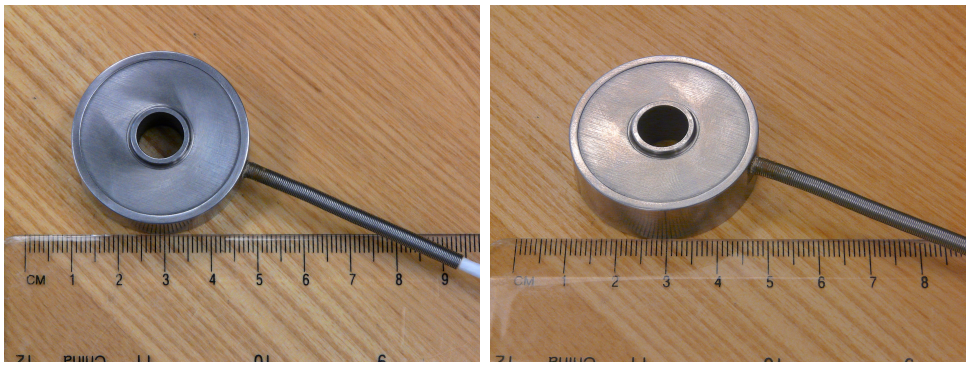

(a) Donut load cell, top view (b) Donut load cell, iso. view

Figure 12: Donut load cell, removed from fixture

variability of the results, improving statistical power.

8.2 Abutment screws

Two types of abutment screws were included in the main study. Both screws have M1.6x0.35 mm thread, and are of similar length, with similar head diameters. The screws are made of Titanium 6Al-4V ASTM F-136 ELI (extra low interstitial), a very common material for abutment screws.

The specific screw types were chosen because they had very similar geometries, except one (screw type 5764) has a tapered seating surface, while the other (screw type 5979) has a flat seating surface (Figure 13, Table 3). As a result, any differences observed between the two screw types should be largely attributable to the screw seating surface geometry (tapered vs. flat). It should be noted that the flat screw has threads formed by thread-rolling, while the tapered screw has cut threads.

Table 3: Screw dimensions. Dimension names correspond to those shown in Figure 8. l_c is the length of the tapered seating surface

	"flat screw" 5979	"tapered screw" 5764
Hex Insert	ST-005-13	ST-005-12
l_h	1.80 mm	2.09 mm
l_c	0 mm	0.49 mm
l_b	1.56 mm	1.62 mm
l_t	2.04 mm	1.34 mm
l_e	2.40 mm	2.40 mm

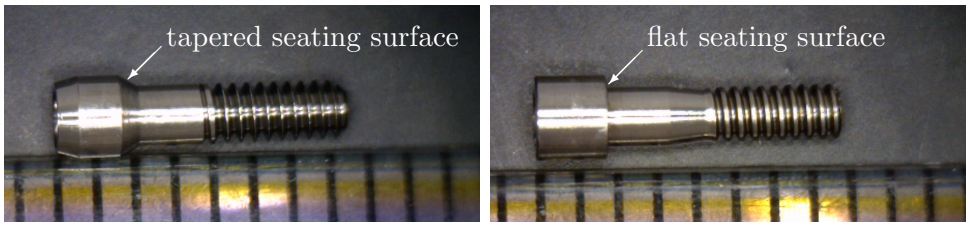

(a) Abutment screw 5764 "tapered screw" (b) Abutment screw 5979 "flat screw"

Figure 13: Abutment screws from main study, on 1 mm graduations

8.3 Simulated Implant Threads and Simulated Abutment Counterbore

The fixture can use specially machined test components to simulate the abutment counterbore (screw seating surface) and the female threads of the implant, or different fixture components can be used to allow the use of actual abutments and modified implants.

For this study, specially designed and machined components were used to simulate the implant threads and the abutment counterbore. The inserts were machined from Titanium 6Al-4V ASTM F-136 ELI (extra low interstitial). This is a common material for both implants and abutments. The components were sourced from a large OEM supplier to the implant industry, and the supplier was instructed to form the internal threads of the threaded insert using a process that they would typically use for dental implants. These inserts are shown in Figure 14.

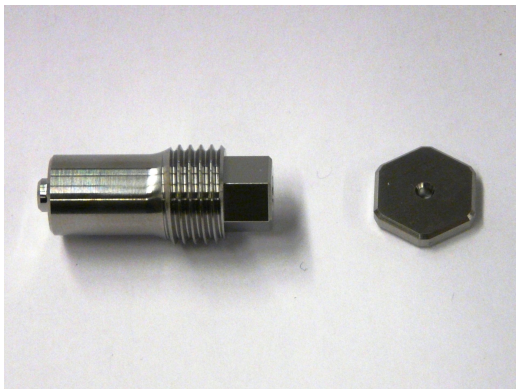

Figure 14: Threaded insert ST-009-M1.6 (left) and hex insert ST-005-12 for tapered screw 5764 (right). Note: hex insert ST-005-13 for flat screw 5979 is not shown

9 Main Study Methods

9.1 Experimental Design

The experimental design is a full-factorial, meaning all combinations of factors and levels are separately tested. This allows studying the effect of each factor separately, as well as the effect of all possible interactions between factors. A full factorial design for this study results in six experimental groups (2 screw contact geometries $\times$ 3 installation protocols = 6 groups).

In order to minimize the disturbance caused by uncontrollable factors, a block-randomized design was chosen. In a block-randomized design, the order of the experimental trials is randomized within a block, rather than within the entire study.

In this case, the block size was chosen to be equal to the number of groups, so that each experimental block would contain exactly one experimental trial from each experimental group. In this way, it is more likely that an external disturbance (such as a string of unusually warm days) would affect each experimental group in a more equal manner, as all groups had a more-or-less equal number of experimental trials exposed to the disturbance. If instead, a fully

randomized design was chosen, it is more likely that the test sequence would include clusters or "runs" of one experimental group, which would mean that the experimental groups are more likely to be unequally affected by external disturbances.

In order to accelerate the pace of the study, most experimental trials were terminated after a two-hour period. However, to get a feel for how the preload loss would continue over time, a smaller number of experimental trials were observed for a twelve-hour period.

A typical day of testing started with two or three two-hour tests, and ended with one twelve-hour test. In order to ensure that an equal number of experimental trials from each group are included in each of the two-hour and twelve-hour studies, separate randomization plans were created for the two-hour and twelve-hour studies (see Appendix G). The two-hour study plan contains approximately 75% of the total experimental trials, and the remaining experimental trials are in the twelve-hour study. This 75/25 split was chosen to correspond to the breakdown of the ideal testing day. In practice, 41 experimental trials were allowed to run for 12 hours, and an additional 98 experimental trials were terminated after 2 hours.

Table 4: Number of experimental trials in each experimental group

	Flat	Tapered
T	23	23
TT	24	23
TLT	23	23

9.2 Cleaning and Handling

Consumable parts (abutment screws, simulated implants, and simulated abutment counterbores) were cleaned once prior to the start of the first experimental trial using an ultrasonic cleaner (Super-Dent Z7, Darby Dental Supply, Jeri-

cho, NY, USA) with an enzymatic cleaning solution (BioSonic, Coltène/Whaledent Inc, Cuyahoga Falls, OH, USA).

Screws were contained in tissue sample cassettes for the ultrasonic cleaning process (Macrosette, Simport Scientific, Beloeil, QC, Canada) (Figure 15). Ten screws were placed into each cassette, and 10–12 loaded cassettes were placed in the basket of the ultrasonic cleaner. Hex inserts and threaded inserts were placed directly in the cleaning basket of the ultrasonic cleaner. No more than 100 hex inserts were cleaned at a time. Cleaning cycles were run for 20 minutes. After components entered the ultrasonic cleaner, components were handled only with clean tools or with non-powdered latex or nitrile gloves for the remainder of the study.

At the conclusion of the ultrasonic cleaning cycle, parts were removed from the cleaner, excess moisture was blown off with filtered shop air, and parts were left to drain and air-dry on industrial towels (WypAll X80, Kimberly-Clark Professional, Roswel, GA, USA). Cleaned parts were placed in clean storage containers until needed. Screws were stored in zip-top bags of ten screws each, hex inserts and threaded inserts were stored in shipping trays with individual wells for each part.

The consumable test components (abutment screw, simulated counterbore, and simulated implant threads) are randomly assigned to one of three groups corresponding to three different installation protocols.

9.3 Test Setup

The full test procedure is provided in Appendix D. An overview of the procedure is provided here.

Tests are conducted in order according to the randomization plan (see Appendix G). A new screw, new simulated abutment counterbore (hex insert),

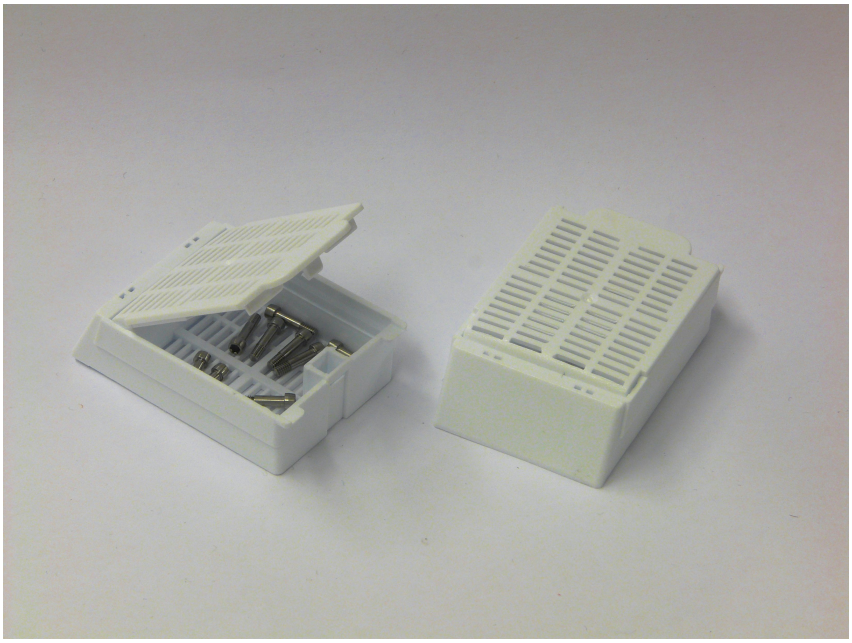

Figure 15: Screws in cleaning cassettes

and simulated abutment threads (threaded insert) are used for each experimental trial. Based on the type of test specified in the randomization plan, new consumable components are retrieved. The simulated implant threads are adjusted such that the grip length of the screw is equal to the target value, based on the screw geometry (see Table 25 in Appendix D for more detail). The target grip length was calculated by requiring each screw to have a nominal length of thread engagement equal to 1.5 $\times$ the nominal diameter of the screw, which works out to 2.4 mm of thread engagement for both of the M1.6 screws included in this study. The adjustment of the simulated implant threads is performed using a Mitutoyo digital height gauge to measure the projection of the threaded insert. The projection is adjusted until it reads within 0.05 mm of the target value.

With the threaded insert adjusted and locked in place, the threaded insert assembly is inserted into the load cell housing, and the hex insert is placed into the load cell housing lid, which is then placed onto the load cell housing.

Figure 16: The Instron 55MT torsion test machine, ready for a test

An abutment screw is then placed into the assembly using plastic tweezers, and threaded into place by hand until initial resistance is felt, then backed off $1/2$ turn.

The entire load cell assembly, with the abutment screw in place, is attached to the tailstock of the Instron 55MT torsion test machine, and the tailstock of the test machine is brought towards the headstock until the abutment screw driver engages the abutment screw. At this point, the tailstock is allowed to slide freely, with a 5 N (1 lb) nominal deadweight providing the force to keep the abutment screw driver engaged with the abutment screw (Figure 16).

The appropriate test procedure file is opened in the Instron Partner software, and specimen identification information is entered for the test. The test sequence is then initiated, and the machine is left undisturbed for the duration of the test (either 2 hours or 12 hours, depending on the randomization plan). At the conclusion of the test, the results are saved to the results database, the abutment screw is loosened using the Instron 55MT power head, and the con-

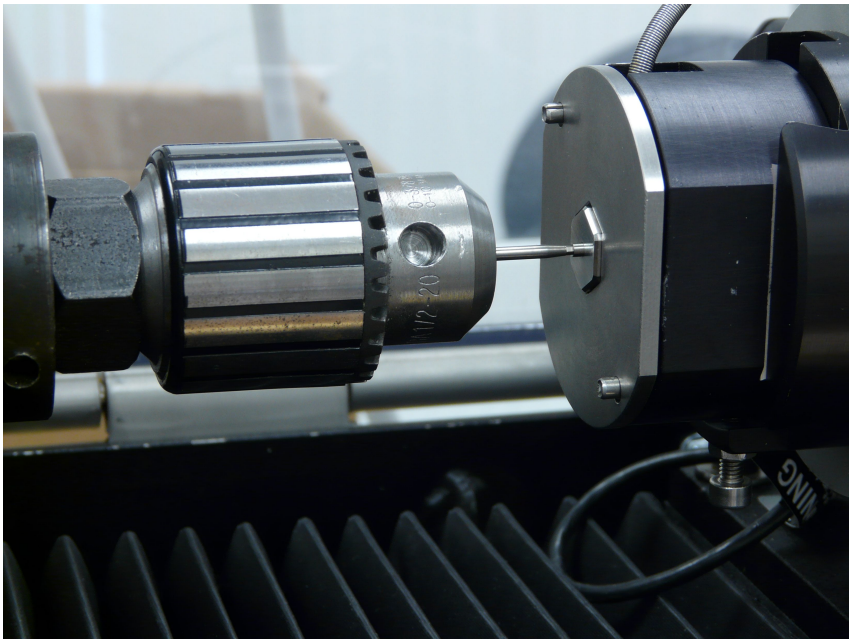

Figure 17: Close-up of the Instron 55MT torsion test machine, showing the abutment screw driver engaging the abutment screw

sumable test components (abutment screw, threaded insert, and hex insert) are individually bagged and labeled.

An outline of the three installation protocols and their associated test procedure is below.

9.4 Group T

This test group is intended to simulate a common installation protocol, whereby the abutment screw is simply torqued to the manufacturer's specified torque level.

New (unused) components are assembled and tightened by the Instron 55MT to the specified installation torque. When the specified installation torque is reached, the applied torque is reduced to zero, and the preload is recorded for a time equal to the study observation period.

An outline of the test program for the T protocol is as follows:

1. Tighten at 6 RPM to 2 N-cm; Data acquisition at 500 Hz, keep every 50th sample (10 sample/sec)
2. Tighten at 2 N-cm/s to 25 N-cm; Data acquisition at 500 Hz, keep every 50th sample (10 sample/sec)
3. Reduce torque at 25 N-cm/s to 0 N-cm; Data acquisition at 500 Hz, keep every 50th sample (10 sample/sec)
4. Hold angle for 15 min; Data acquisition at 500 Hz, keep every 50th sample (10 sample/sec)
5. Hold angle for 11.75 hr; Data acquisition at 10 Hz, keep every 300th sample (2 sample/min)

9.5 Group TT

This test group is intended to simulate one commonly recommended installation protocol, whereby the abutment screw is re-torqued 10 minutes after the initial torque application. A reason that is commonly cited for using this protocol is that the re-tightening after 10 minutes helps to compensate for initial preload loss.

New (unused) components are assembled and tightened by the Instron 55MT to the specified installation torque. When the specified installation torque is reached, the applied torque is reduced to zero, and the preload is recorded for 10 minutes. After 10 minutes, the applied torque is increased until the specified application torque is reached. When the specified installation torque is reached, the applied torque is again reduced to zero, and the preload is recorded for a time equal to the study observation period.

An outline of the test program for the TT protocol is as follows:

1. Tighten at 6 RPM to 2 N-cm; Data acquisition at 500 Hz, keep every 50th

sample (10 sample/sec)

2. Tighten at 2 N-cm/s to 25 N-cm; Data acquisition at 500 Hz, keep every 50th sample (10 sample/sec)
3. Reduce torque at 25 N-cm/s to 0 N-cm; Data acquisition at 500 Hz, keep every 50th sample (10 sample/sec)
4. Wait 10 minutes; Data acquisition at 500 Hz, keep every 50th sample (10 sample/sec)
5. Tighten at 2 N-cm/s to 25 N-cm; Data acquisition at 500 Hz, keep every 50th sample (10 sample/sec)
6. Reduce torque at 25 N-cm/s to 0 N-cm; Data acquisition at 500 Hz, keep every 50th sample (10 sample/sec)
7. Hold angle for 15 min; Data acquisition at 500 Hz, keep every 50th sample (10 sample/sec)
8. Hold angle for 11.75 hr; Data acquisition at 10 Hz, keep every 300th sample (2 sample/min)

9.6 Group TLT

This test group is intended to simulate an alternate installation protocol, whereby 10 minutes after the initial torque application, the abutment screw is loosened one half turn, then re-tightened to the specified installation torque. It is hypothesized that the additional sliding wear caused by the loosening and re-tightening would cause a greater degree of surface smoothing than the Group T or Group TT protocol, which could lead to reduced potential for initial preload loss.

New (unused) components are assembled and tightened by the Instron 55MT to the specified installation torque. When the specified installation

torque is reached, the applied torque is reduced to zero, and the preload is recorded for 10 minutes. After 10 minutes, the abutment screw is turned 180° counterclockwise to loosen, then immediately the applied torque is increased in the clockwise direction until the specified application torque is reached. When the specified installation torque is reached, the applied torque is again reduced to zero, and the preload is recorded for a time equal to the study observation period.

An outline of the test program for the TLT protocol is as follows:

1. Tighten at 6 RPM to 2 N-cm; Data acquisition at 500 Hz, keep every 50th sample (10 sample/sec)
2. Tighten at 2 N-cm/s to 25 N-cm; Data acquisition at 500 Hz, keep every 50th sample (10 sample/sec)
3. Reduce torque at 25 N-cm/s to 0 N-cm; Data acquisition at 500 Hz, keep every 50th sample (10 sample/sec)
4. Wait 10 minutes, mark angle; Data acquisition at 500 Hz, keep every 50th sample (10 sample/sec)
5. Loosen ½ turn relative to marked angle,at XX RPM; Data acquisition at 500 Hz, keep every 50th sample (10 sample/sec)
6. Tighten at 6 RPM to 2 N-cm; Data acquisition at 500 Hz, keep every 50th sample (10 sample/sec)
7. Tighten at 2 N-cm/s to 25 N-cm; Data acquisition at 500 Hz, keep every 50th sample (10 sample/sec)
8. Reduce torque at 25 N-cm/s to 0 N-cm; Data acquisition at 500 Hz, keep every 50th sample (10 sample/sec)
9. Hold angle for 15 min; Data acquisition at 500 Hz, keep every 50th sample (10 sample/sec)

10. Hold angle for 11.75 hr; Data acquisition at 10 Hz, keep every 300th sample (2 sample/min)

9.7 Statistical Methods

Following completion of the experimental trials, the data were analyzed using R [13]. Key metrics evaluated include:

Initial Preload The peak preload generated during the last tightening event.

Residual Preload The preload remaining in the joint after some defined settling period

Absolute Preload Loss The difference (expressed in Newtons) between the residual preload and the peak preload generated during tightening

Relative Preload Loss The difference between the peak preload generated during tightening and the residual preload (expressed as a percentage of peak preload)

For the T group, preload loss was calculated by comparing the maximum preload measured during the test (P_{max1}) with the preload measured during the test 120 min after peak torque was reached during tightening (P_{120}).

Absolute preload loss was calculated as

$$P_{max1} - P_{120}$$

Relative preload loss was calculated as

$$\frac{P_{max1} - P_{120}}{P_{max1}} \times 100\%$$

and expressed as a percentage.

For the TT and TLT groups, preload loss was calculated by comparing the maximum preload measured during the *second* tightening (P_{max2}) with the preload measured during the test 120 min after peak torque was reached during the *second* tightening (P_{120}).

Absolute preload loss was calculated as

$$P_{max2} - P_{120}$$

Relative preload loss was calculated as

$$\frac{P_{max2} - P_{120}}{P_{max2}} \times 100\%$$

and expressed as a percentage.

Note that the that the peak preload measured during the second tightening (P_{max2}) may in some cases be less than the peak preload measured during the first tightening (P_{max1}).

Examination of the experimental data showed that a typical two-way ANOVA analysis was contraindicated due to the unequal variance between the experimental groups, and the non-normality of the residuals of the linear model underlying the ANOVA.[3] These factors constitute violations of the assumptions of ANOVA techniques. Accordingly, non-parametric statistical methods were used to evaluate the experimental results.

Non-parametric statistics, in contrast to parametric statistics, are not based on summary statistics like means and standard deviations, and do not rely on assumptions that the data follow any specific distribution (e.g. the Gaussian distribution). They are often based upon ordinal, or ranked data, rather than upon the actual variate data itself. As a result, non-parametric statistics

[3]Non-normality was assessed using a Shapiro-Wilk normality test on the residuals.

tend to be more robust to the presence of outliers. The downside of non-parametric statistics is that they tend to have less statistical power than their parametric counterparts, with the consequence being that larger sample sizes are sometimes required to find a significant result.

This study makes use of The Kruskal-Wallis one-way analysis of variance, and the Wilcoxon rank sum test. The Kruskal-Wallis test is a non-parametric alternative to a one-way ANOVA, and the Wilcoxon rank sum test is a non-parametric alternative to an unpaired t-test. The Kruskal-Wallis test and Wilcoxon rank sum test are considered robust to non-normal data and unequal variance.

In this study a Wilcoxon rank sum test (equivalent to a Mann-Whitney test) was used to evaluate the difference in each computed metric (i.e. initial preload, residual preload, absolute preload loss, and relative preload loss) between the two screw geometries, and two Kruskal-Wallis one-way analysis of variance tests were used to to determine whether installation protocol had an effect on the above metrics within each of the two screw geometries. Where the Kruskal-Wallis one-way analysis of variance found a statistically significant effect, post-hoc pairwise Wilcoxon rank sum tests were used to perform pairwise comparison between different installation protocols within each screw type. The Holm method was used to correct the p values from these pairwise tests for multiple comparisons [8].

9.8 Wilcoxon Rank Sum Example Calculation

What follows is two worked examples for calculation of the Wilcoxon rank sum test. This test is a non-parametric alternative to an unpaired two-sample t-test. These examples will test the null hypothesis that that the distribution

of values in group A is the same as that of group B,

$$H_0 : A = B$$

against a two-sided alternate hypothesis that there is a shift between groups A and B

$$H_1 : A \neq B$$

The first example is based on a data set corresponding to the null hypothesis, that the distribution of values in group A is the same as that of group B. Such a data set is shown in Figure 18.[4]

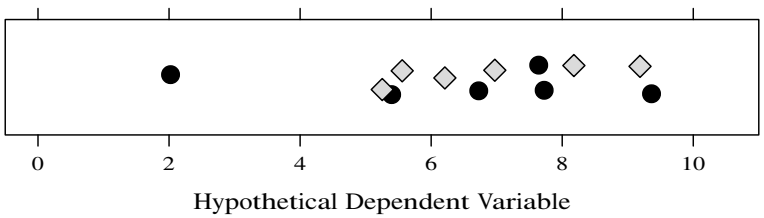

Figure 18: Two-sample univariate data corresponding to the null hypothesis

To compute the Wilcoxon rank sum, the data must first be rank-transformed. The result of rank transforming the data is shown in Table 5.

The Wilcoxon rank sum test statistic has been defined differently in various sources, but one common definition is to simply sum the ranks of the data within each group. So for the data shown in Table 5:

$$W_\bullet = 1 + 3 + 6 + 8 + 9 + 12 = 39$$
$$W_\diamond = 2 + 4 + 5 + 7 + 10 + 11 = 39$$

Note that in this case, the rank sums are equal for the two groups. This is

[4]To form the data set for the null condition, 12 random values were drawn from one normal distribution, with the first six random values being assigned to one group, and the next six values being assigned to the other group

Table 5: Example Wilcoxon rank sum data, null condition

Value	Rank	Group
2.02	1	●
5.25	2	◇
5.40	3	●
5.56	4	◇
6.21	5	◇
6.73	6	●
6.97	7	◇
7.64	8	●
7.72	9	●
8.18	10	◇
9.19	11	◇
9.36	12	●

somewhat intuitive: if there is no location shift between groups, there ought to be some central-tendency of the rank sums. In this case, the rank sums came out to be exactly equal.

The next example is based on a data set where there is a difference in location between the groups, and therefore the null hypothesis should be rejected. Such a data set is shown in Figure 19.[5]

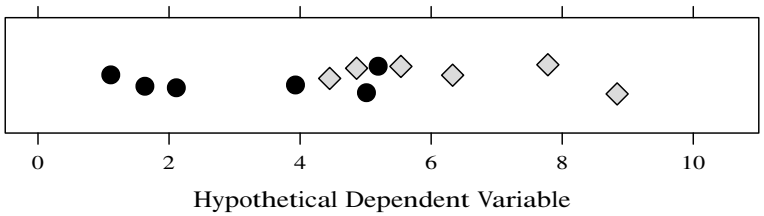

Figure 19: Two-sample univariate data corresponding to the alternate hypothesis

Again, to calculate the Wilcoxon rank sum, the data must be rank-transformed. The result is shown in Table 6.

[5]To form the data set for the alternate condition, six (6) random values were drawn from a normal distribution with a mean of two (2), and assigned to the first group; and six (6) random values were drawn from a normal distribution with a mean of seven (7), and assigned to the second group.

Table 6: Example Wilcoxon rank sum data, alternate (non-null) condition

Value	Rank	Group
1.11	1	•
1.63	2	•
2.11	3	•
3.93	4	•
4.45	5	◇
4.86	6	◇
5.01	7	•
5.19	8	•
5.54	9	◇
6.33	10	◇
7.78	11	◇
8.84	12	◇

The Wilcoxon rank sum can then be computed:

$$W_{\bullet} = 1 + 2 + 3 + 4 + 7 + 8 = 25$$

$$W_{\diamond} = 5 + 6 + 9 + 10 + 11 + 12 = 53$$

Note that in this case the rank sums for the two groups are not equal. Again, this is somewhat intuitive: if there is a location shift between the two groups, the rank sums of those two groups should diverge. The critical value of the Wilcoxon rank sum can now be retreived from a table to determine whether the observed difference is a statistically significant one.

For a two-sample test with $n_A = n_B = 6$, and a significance level of $\alpha = .05$, the critical value of the Wilcoxon rank sum for the lower tail is 28.[6] If the smaller of our two computed Wilcoxon rank-sums is equal to or less than 28, then the test indicates a significant difference. In the case of the second example, $W_{\bullet} = 25 \leq 28$, so the null hypothesis is rejected.

It is worth noting that the W values reported in this thesis are computed by the `wilcox.test` function of R, which uses an alternate definition of the test

[6]A table of critical Wilcoxon rank sum values, as well as further information on the Wilcoxon rank sum test is available at `https://www.stat.auckland.ac.nz/~wild/ChanceEnc/Ch10.wilcoxon.pdf`

statistic, one that is closer to the Mann-Whitney U-test, though the principle is the same as that presented in the preceding examples [13].

The Kruskal-Wallis one-way analysis of variance can be thought of as an extension of the Wilcoxon rank sum method to three or more samples.

10 Roughness Measurement Methods

After the conclusion of the main study, ten (10) unused flat screws, plus ten (10) randomly selected flat screws from each of the three experimental installation protocols were subjected roughness measurement ($n = 40$) to evaluate the effect of installation protocol on surface roughness, as surface finish is believed to be a significant factor in embedment relaxation [2]. Roughness measurements were conducted using a Mitutoyo CS3200S4 profilometer and Formtracepak6000 software (Mitutoyo America Corporation, Aurora, IL, USA, Figure 20). The tapered screw was not included in the roughness evaluation due to the additional complexity that would have been involved in taking roughness measurements on the conical seating surface of the screw.

Measuring on this small surface presented some challenges. The stylus of the profilometer was too large to clear the screw shank and still make contact with the underhead surface. In order to address this issue, the screw was inclined 31° from vertical, which provided clearance for the 60° point of the stylus (Figure 20b). As a result, the measurement results are not "true" R_a or W_a (average roughness and average waviness, respectively), since they were not measured normal to the surface of the screw. Nonetheless, they are still valuable in that they allow for relative comparison between experimental groups.

Measurements were taken over a 0.8 mm sample length on the underside of

(a) Profilometer, as used to measure the roughness of the flat screws

(b) Close-up of profilometer and fixturing, showing stylus tracing the screw seating surface

Figure 20: Roughness measurement apparatus

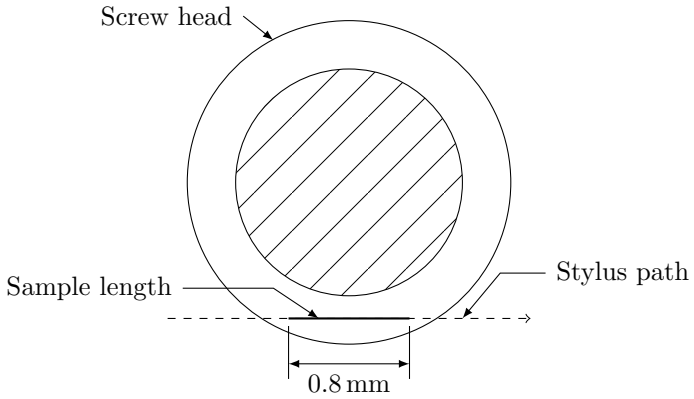

Figure 21: Location of roughness measurement sample length

the screw head (Figure 21).

11 Scanning Electron Microscopy Methods

After the conclusion of the main study, one (1) unused flat screw, plus one (1) randomly selected flat screw and matching simulated abutment counterbore from each of the three experimental installation protocols (a total of $n = 4$ screws and $n = 3$ simulated counterbores) were sent for scanning electron microscopy (SEM) to evaluate the effect of installation protocol on surface condition at the contact surfaces.

Scanning electron microscopy was performed using a Topcon SM-510 scanning electron microscope (Topcon Corporation, Itabashi, Tokyo, Japan), with a lanthanum hexaboride (LaB6) filament. The samples were mounted to an aluminum stub using double-sided carbon tape. Since the samples were electrically conductive, no sputter-coating or additional sample preparation was required. The samples were tilted 45° towards the detector. Secondary electron images at various magnifications were collected using a 20 kV accelerating voltage. A small final aperture (50 micron), small spot size, and long working distance (approximately 25 mm) were used to improve depth of field.

12 White Light Inferferometry Methods

In another attempt to characterize the seating surface of the screw and the mating counterbore surface, one screw and one hex insert from each installation protocol for the flat screw were subjected to white light interferometry using a Zygo machine.

13 Main Study Results

Following completion of the experimental trials, the data were analyzed using R [13]. Key metrics evaluated include:

Initial Preload The peak preload generated during the last tightening event.

Residual Preload The preload remaining in the joint after some defined settling period

Absolute Preload Loss The difference (expressed in Newtons) between the residual preload and the peak preload generated during tightening

Relative Preload Loss The difference between the peak preload generated during tightening and the residual preload (expressed as a percentage of peak preload)

One test was removed from the analysis due to procedural error during the test setup. One test was removed from the analysis because the test sequence was stopped prematurely. One additional test was removed from the analysis due to an unexplained increase in observed preload around 40 minutes into the test sequence.

Table 7: Number of experimental trials in each experimental group

	Flat	Tapered
T	23	23
TT	24	23
TLT	23	23

13.1 Initial Preload

As peak installation torque was held constant across all experimental groups, by examining the initial preload generated upon the final tightening (P_1 for the T group, P_2 for the TT and TLT group), one can observe the impact of the two retightening protocols on the torque/preload relationship.

Figure 22 demonstrates that the initial preload is considerably higher for the flat screw with the rolled threads than for the tapered screw with the cut threads, though the peak installation torque is the same for both screws. The torque applied to a screw head during tightening gets reacted by several different mechanisms: friction under the screw head, friction at the screw threads, and elongation of the screw. It is this elongation of the screw that creates preload [2]. The tapered screw head uses a larger fraction of the applied torque to overcome friction under the screw head, due to a wedging effect created by

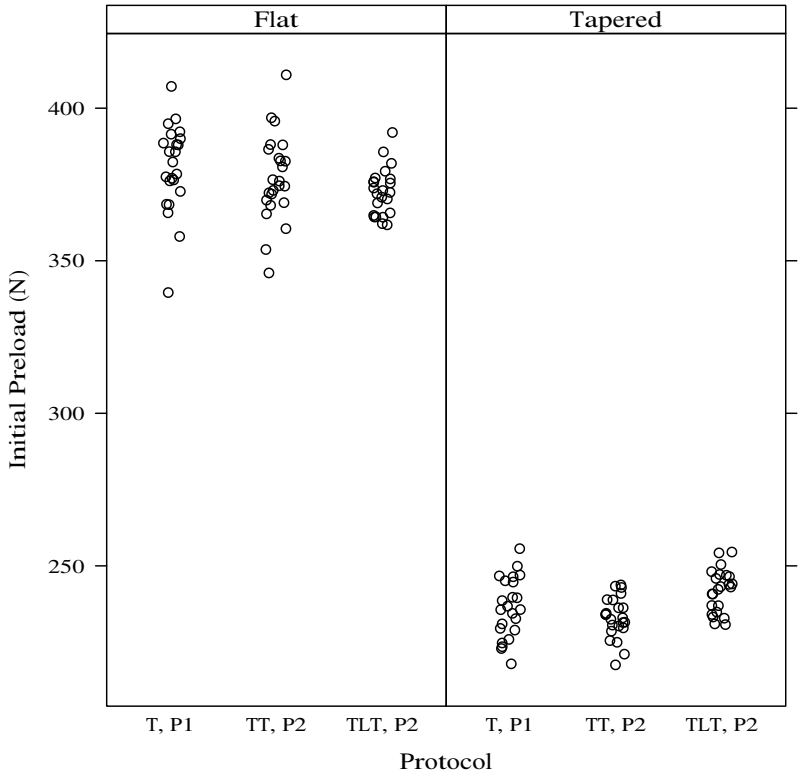

Figure 22: Initial preload

the taper. This leaves less applied torque available to create elongation in the screw, and therefore less preload is generated in the tapered screw.

Table 8: Mean initial preload, with 95% confidence interval

	Flat	Tapered
T, P1	380.4 ± 6.2 N	236.2 ± 4.3 N
TT, P2	377.0 ± 5.9 N	233.1 ± 3.0 N
TLT, P2	372.6 ± 3.3 N	241.9 ± 3.0 N

A Wilcoxon rank sum test confirms that the observed difference in initial preload between the tapered screw (μ = 237.0 N, 95% CI [235.0 N, 239.1 N]) and the flat screw (μ = 376.7 N, 95% CI [373.6 N, 379.7 N]) is statistically significant ($W = 0$, p = 2.7E-24).

The Kruskal-Wallis one-way analysis of variance shows that the installation protocol did have an effect on the initial preload for the tapered screw (H =

12.4, $df = 2$, $p = 0.00202$), and the flat screw ($H = 7.43$, $df = 2$, $p = 0.0243$).

For the tapered screw, the T protocol (control) had a mean initial preload of 236.2 N, 95% CI [232.0 N, 240.5 N]. The initial preload generated by the TT protocol ($\mu = 233.1$ N, 95% CI [230.1 N, 236.0 N]) was not shown to be significantly different from the T protocol ($W = 262$, $p = 0.256$). The initial preload generated by the TLT protocol ($\mu = 241.9$ N, 95% CI [238.8 N, 244.9 N]) was shown to be 4% higher than the TT protocol, and this difference was found to be statistically significant ($W = 150$, $p = 0.00044$), but the initial preload generated by the TLT protocol was not shown to be significantly different from the T protocol ($W = 167$, $p = 0.0998$) (Tables 8, 9).

Table 9: Pairwise Wilcoxon rank sum test p values (with Holm correction for multiple comparisons): initial preload, tapered screw

	T, P1	TT, P2
TT, P2	0.26	
TLT, P2	0.1	0.00044

For the flat screw, the T protocol (control) had the highest mean initial preload ($\mu = 380.4$ N, 95% CI [374.2 N, 386.6 N]). The initial preload generated by the TT protocol ($\mu = 377.0$ N, 95% CI [371.1 N, 382.9 N]) was not shown to be significantly different from the T protocol ($W = 252$, $p = 0.317$). The initial preload generated by the TLT protocol ($\mu = 372.6$ N, 95% CI [369.2 N, 375.9 N]) was shown to be 2% lower than the T protocol, and this difference was found to be statistically significant ($W = 248.5$, $p = 0.317$). No significant difference in initial preload was found between the TT protocol and the TLT protocol ($W = 289$, $p = 0.317$) (Tables 8, 10).

For the TT protocol, an additional metric, preload rise, was calculated in an attempt to directly observe the effect of the simple retightening. The preload rise is defined as the difference between the peak preload generated during the second tightening and the load immediately prior to the second

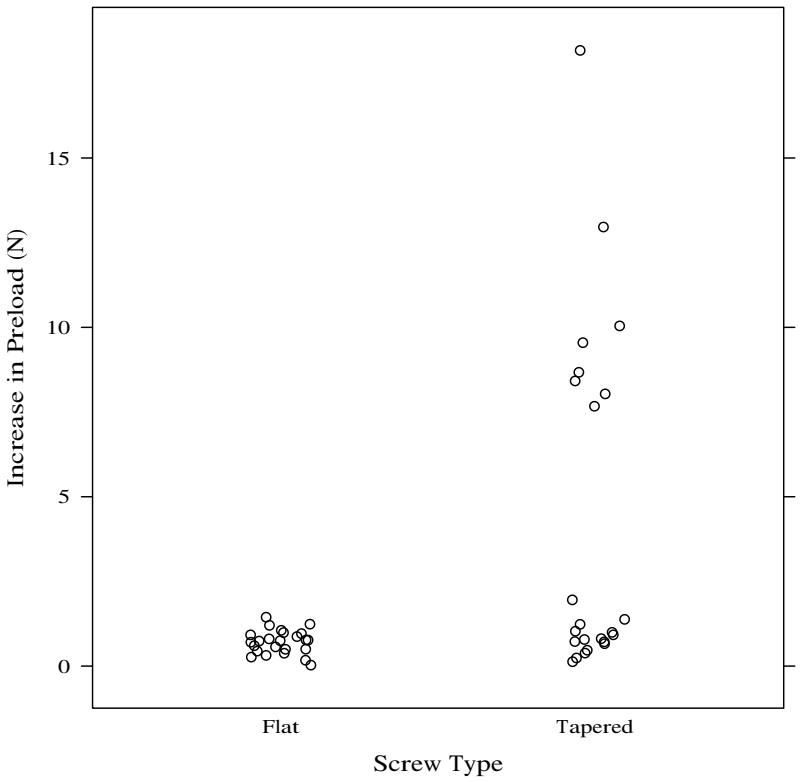

Figure 23: Preload rise on second tightening, TT group

tightening. For the flat screw, the range of preload rise was 0–1.4 N. For the tapered screw, the range of preload rise was 0.1–18.2 N.

Table 10: Pairwise Wilcoxon rank sum test p values (with Holm correction for multiple comparisons): initial preload, flat screw

	T, P1	TT, P2
TT, P2	0.32	
TLT, P2	0.016	0.32

13.2 Residual Preload

The residual preload is defined as the preload present in the joint 120 min after the last tightening intervention. Figure 24 demonstrates that, similar to the initial preload, the residual preload is considerably higher for the flat screw than for the tapered screw.

Table 11: Mean residual preload, with 95% confidence interval

	Flat	Tapered
T	372.7 ± 6.8 N	228.3 ± 4.7 N
TT	374.1 ± 6.0 N	230.6 ± 3.1 N
TLT	367.2 ± 3.5 N	237.6 ± 3.2 N

A Wilcoxon rank sum test confirms that the observed difference in residual preload between the tapered screw with rolled threads ($\mu = 232.2$ N, 95% CI [229.9 N, 234.5 N]) and the flat screw with cut threads ($\mu = 371.4$ N, 95% CI [368.2 N, 374.6 N]) is statistically significant ($W = 0$, $p = 2.7\text{E-}24$).

The Kruskal-Wallis one-way analysis of variance shows that the installation protocol did have an effect on residual preload for the tapered screw ($H = 11.7$, $df = 2$, $p = 0.00287$), but statistical significance was not found for the flat screw ($H = 5.15$, $df = 2$, $p = 0.0761$).

For the tapered screw, the T protocol (control) had the lowest mean residual preload ($\mu = 228.3$ N, 95% CI [223.5 N, 233.0 N]). The residual preload generated by the TT protocol ($\mu = 230.6$ N, 95% CI [227.6 N, 233.7 N]) was not shown to be significantly different from the T protocol ($W = 217$, $p = 0.305$). The highest mean residual preload was generated by the TLT protocol ($\mu = 237.6$ N, 95% CI [234.4 N, 240.9 N]) which was 4% higher than the T protocol, and this difference was found to be statistically significant ($W = 129$, $p = 0.00735$); and 3% higher than the TT protocol, and this difference was found to be statistically significant ($W = 138$, $p = 0.00975$) (Tables 11, 12).

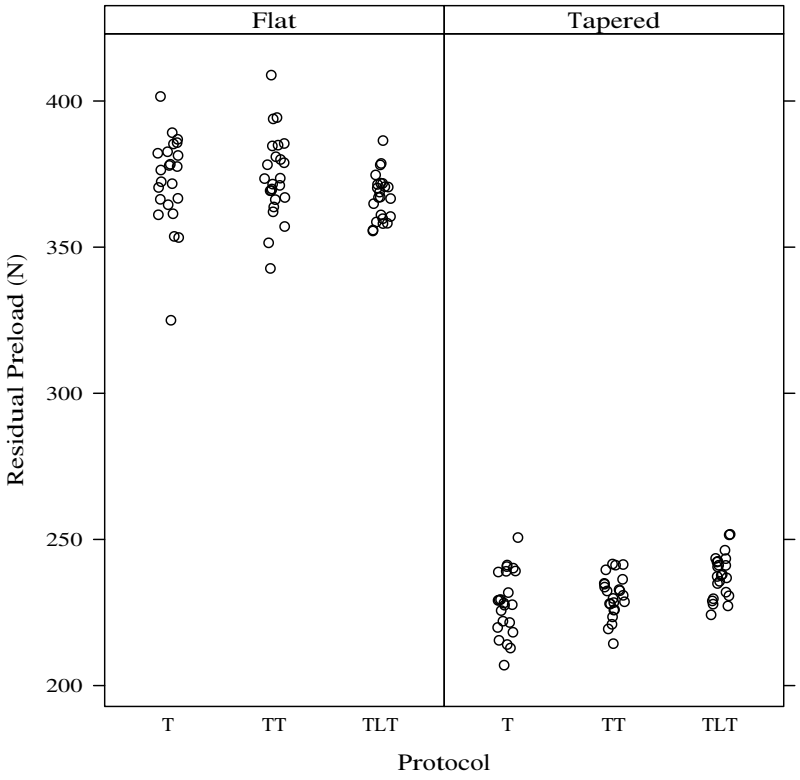

Figure 24: Residual preload after 120 min

Table 12: Pairwise Wilcoxon rank sum test p values (with Holm correction for multiple comparisons): residual preload, tapered screw

	T	TT
TT	0.3	
TLT	0.0073	0.0097

For the flat screw, no significant differences were found in residual preload between the various installation protocols (T↔TT: $W = 278$, $p = 0.975$; T↔TLT: $W = 353$, $p = 0.145$; TT↔TLT: $W = 369$, $p = 0.145$) (Tables 11, 13).

Table 13: Pairwise Wilcoxon rank sum test p values (with Holm correction for multiple comparisons): residual preload, flat screw

	T	TT
TT	0.97	
TLT	0.15	0.15

Tests for equivalence of variance were conducted to determine if any of the re-tightening protocols could influence the variability in residual preload.

Prior to testing for equivalence of variance, the residual preload within each of the experimental groups was checked for normality using a Shapiro-Wilk normality test. In all cases, the null hypothesis that the data came from a normal distribution could not be rejected. Therefore, the normality assumption of the F-test is not violated, and the F-test can be used to check for differences in variance between groups.

For the 5764 screw, which has a tapered seating surface, there was a significant difference in residual preload variance between the T group and the TT group, with the TT group displaying lower variance than the T group ($p = 0.0496$). All other pairwise comparisons for the tapered screw failed to show a statistically significant difference in variance of residual preload (Table 14).

For the 5979 screw, which has a flat seating surface, the TLT protocol displayed significantly lower residual preload variance than the T protocol ($p = 0.0027$) and the TT protocol ($p = 0.0087$). No statistically significant difference in residual preload variance was found between the T protocol and TT protocol (Table 15).

Table 14: Pairwise F-test p values: residual preload, tapered screw

	T	TT
TT	0.0496	
TLT	0.0786	0.8318

Table 15: Pairwise F-test p values: residual preload, flat screw

	T	TT
TT	0.6644	
TLT	0.0027	0.0087

13.3 Relative Preload Loss

The relative preload loss is defined as the difference between the initial preload (i.e. the peak preload generated during the final tightening) and the residual preload, and is expressed as a percentage of initial preload. Significant within-group variability of relative preload loss is evident in Figure 25.

A Wilcoxon rank sum test finds that the difference in relative preload loss between the tapered screw (μ = 2.1%, 95% CI [1.8%, 2.4%]) and the flat screw (μ = 1.4%, 95% CI [1.2%, 1.6%]) is statistically significant ($W = 3211$, $p = 0.0008$).

The Kruskal-Wallis one-way analysis of variance shows that the installation protocol did have an effect on relative preload loss for the tapered screw (H = 47.6, df = 2, p = 4.7E-11), and the flat screw (H = 50.4, df = 2, p = 1.13E-11).

Table 16: Mean relative preload loss, with 95% confidence interval

	Flat	Tapered
T	$\mu = 2.0\% \pm 0.3\%$	$\mu = 3.4\% \pm 0.6\%$
TT	$\mu = 0.8\% \pm 0.1\%$	$\mu = 1.0\% \pm 0.2\%$
TLT	$\mu = 1.4\% \pm 0.2\%$	$\mu = 1.8\% \pm 0.2\%$

For the tapered screw, the T protocol (control) had the highest mean relative preload loss (μ = 3.4%, 95% CI [2.8%, 3.9%]). The TT protocol had the lowest relative preload loss (μ = 1.0%, 95% CI [0.9%, 1.2%]), a 69% reduction compared to the T protocol. This difference was found to be statistically significant ($W = 525$, p = 8.74E-12). The TLT protocol (μ = 1.8%, 95% CI [1.5%, 2.0%]), provided a 48% reduction in relative preload loss compared to the T protocol. This difference was found to be statistically significant ($W = 481$, p = 4.15E-07). The difference between the TT and the TLT protocols was also found to be statistically significant ($W = 64$, p = 2.42E-06) (Tables 16,

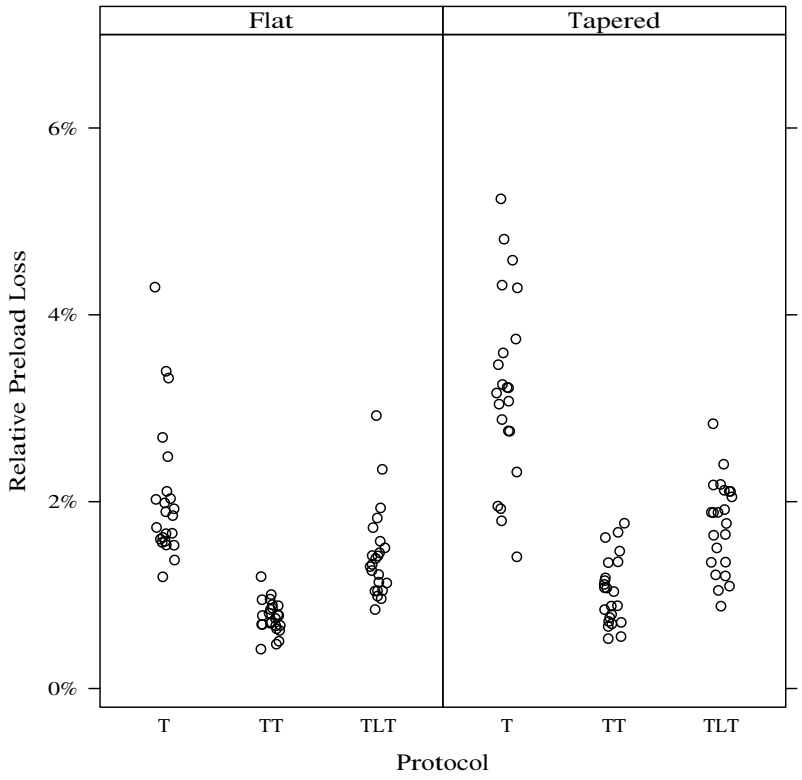

Figure 25: Relative load loss after 2 hours

17).

Table 17: Pairwise Wilcoxon rank sum test p values (with Holm correction for multiple comparisons): relative preload loss, tapered screw

	T	TT
TT	8.7E-12	
TLT	4.1E-07	2.4E-06

For the flat screw, the ordinal ranking of mean relative preload loss by protocol is the same. The T protocol (control) again had the highest mean relative preload loss ($\mu = 2.0\%$, 95% CI [1.7%, 2.4%]). The TT protocol had the lowest relative preload loss ($\mu = 0.8\%$, 95% CI [0.7%, 0.8%]), a 63% reduction compared to the T protocol. This difference was found to be statistically significant ($W = 551$, $p = 7.44\text{E-}13$). The TLT protocol ($\mu = 1.4\%$, 95% CI [1.2%, 1.6%]), provided a 30% reduction in relative preload loss compared to the T protocol. This difference was found to be statistically significant ($W = 436$, $p = 8.65\text{E-}05$). The difference between the TT and the TLT protocols was also found to be statistically significant ($W = 17$, $p = 3.01\text{E-}10$) (Tables 16, 18).

Table 18: Pairwise Wilcoxon rank sum test p values (with Holm correction for multiple comparisons): relative preload loss, flat screw

	T	TT
TT	7.4E-13	
TLT	8.7E-05	3E-10

13.4 Absolute Preload Loss

The absolute preload loss is defined as the difference between the initial preload (i.e. the peak preload generated during the final tightening) and the residual preload, and is expressed in Newtons. Significant within-group variability of absolute preload loss is evident in Figure 26.

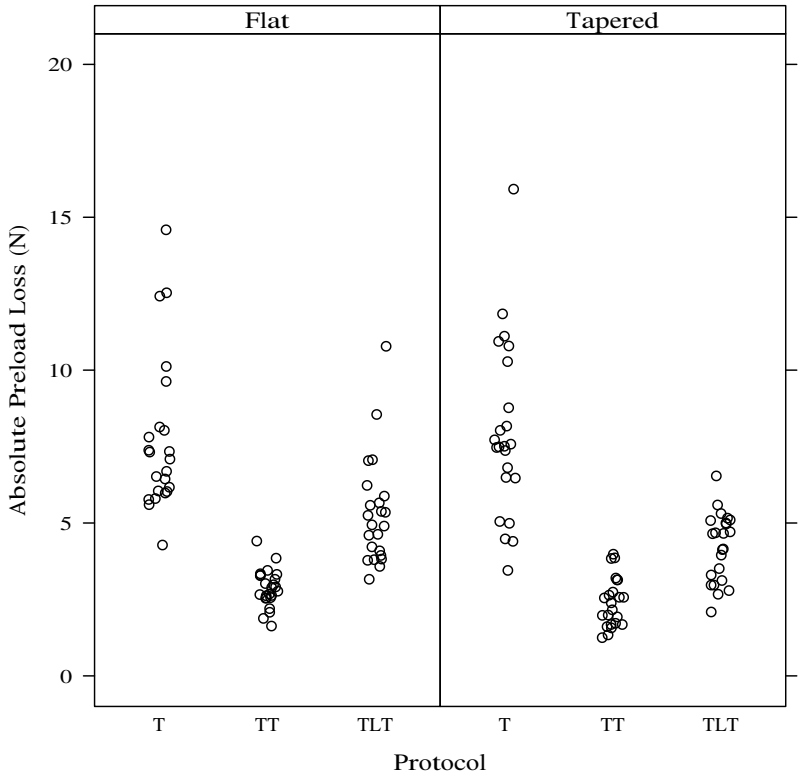

Figure 26: Absolute load loss after 2 hours

Table 19: Mean absolute preload loss, with 95% confidence interval

	Flat	Tapered
T	$7.7 \pm 1.1\,\mathrm{N}$	$8.0 \pm 1.2\,\mathrm{N}$
TT	$2.9 \pm 0.3\,\mathrm{N}$	$2.4 \pm 0.4\,\mathrm{N}$
TLT	$5.3 \pm 0.8\,\mathrm{N}$	$4.2 \pm 0.5\,\mathrm{N}$

A Wilcoxon rank sum test does not find a statistically significant difference in absolute preload loss between the tapered screw ($\mu = 4.9\,\text{N}$, 95% CI [4.2 N, 5.6 N]) and the flat screw ($\mu = 5.3\,\text{N}$, 95% CI [4.6 N, 5.9 N]) ($W = 2118$, $p = 0.21$).

The Kruskal-Wallis one-way analysis of variance shows that the installation protocol did have an effect on absolute preload loss for the tapered screw ($H = 48.3$, $df = 2$, $p = 3.18\text{E-}11$), and the flat screw ($H = 51$, $df = 2$, $p = 8.3\text{E-}12$).

For the tapered screw, the T protocol (control) had the highest mean absolute preload loss ($\mu = 8.0\,\text{N}$, 95% CI [6.7 N, 9.2 N]). The lowest absolute preload loss was generated by the TT protocol ($\mu = 2.4\,\text{N}$, 95% CI [2.1 N, 2.8 N]), a reduction of 70% relative to the T protocol. This difference was shown to be statistically significant ($W = 526$, $p = 2.93\text{E-}08$). The absolute preload loss of the TLT protocol ($\mu = 4.2\,\text{N}$, 95% CI [3.7 N, 4.7 N]) showed a 47% reduction in absolute preload loss compared to the T protocol, and this difference was found to be statistically significant ($W = 474$, $p = 5.74\text{E-}06$). The difference in absolute preload loss between the TT and TLT protocols was also found to be statistically significant ($W = 51$, $p = 5.74\text{E-}06$) (Tables 19, 20).

Table 20: Pairwise Wilcoxon rank sum test p values (with Holm correction for multiple comparisons): absolute preload loss, tapered screw

	T	TT
TT	2.9E-08	
TLT	5.7E-06	5.7E-06

The same ordinal ranking of protocols by absolute preload loss was observed for the flat screw. For the flat screw, the T protocol (control) had the highest mean absolute preload loss ($\mu = 7.7\,\text{N}$, 95% CI [6.6 N, 8.8 N]). The lowest absolute preload loss was generated by the TT protocol ($\mu = 2.9\,\text{N}$, 95% CI

[2.6 N, 3.1 N]), a reduction of 63% relative to the T protocol. This difference was shown to be statistically significant ($W = 551$, $p = 7.44\text{E-}13$). The absolute preload loss of the TLT protocol ($\mu = 5.3$ N, 95% CI [4.6 N, 6.1 N]) showed a 31% reduction in absolute preload loss compared to the T protocol, and this difference was found to be statistically significant ($W = 447$, $p = 2.49\text{E-}05$). The difference in absolute preload loss between the TT and TLT protocols was also found to be statistically significant ($W = 19$, $p = 5.18\text{E-}10$) (Tables 19, 21).

Table 21: Pairwise Wilcoxon rank sum test p values (with Holm correction for multiple comparisons): absolute preload loss, flat screw

	T	TT
TT	7.4E-13	
TLT	2.5E-05	5.2E-10

14 Roughness Measurement Results

Roughness measurements were taken using a profilometer in an attempt to determine whether installation protocol had an effect on the surface finish of the contact surfaces of the screw. Only the flat screw was included in the roughness measurement study.

As the measurements were taken with the stylus inclined at a 31°angle to the screw contact surface, the absolute magnitude of the Ra values reported in Figure 27 and Table 22 are not a true indication of the actual surface roughness, but as the objective is to provide a means for comparison between installation protocols, the reported Ra values are still diagnostically valuable.

Immediately evident in Figure 27 is the large discrepancy between the Ra values for unused screws and the screws that had been subjected to one of the experimental installation protocols.

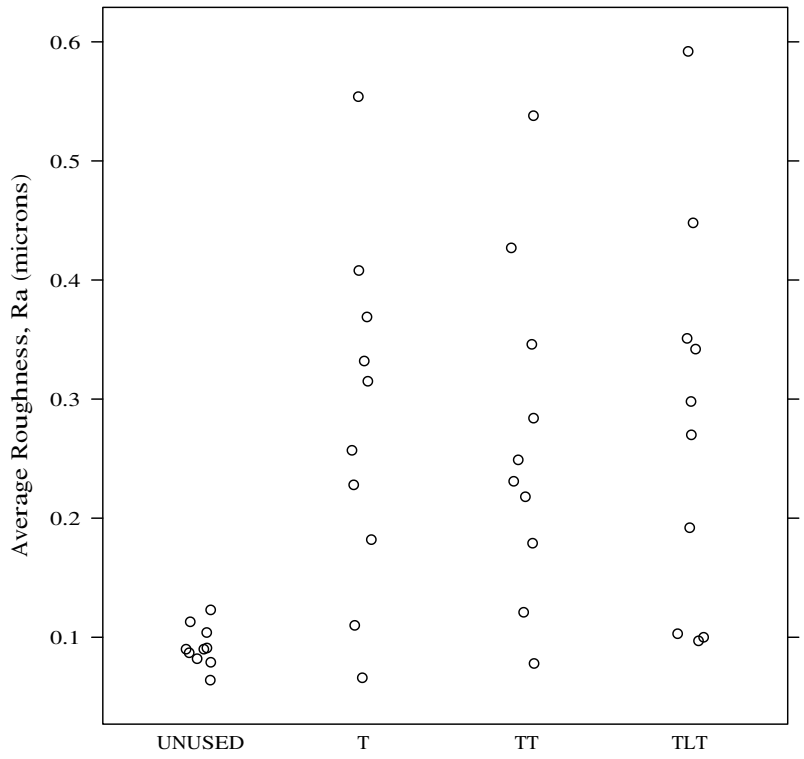

Figure 27: Ra (as measured) by protocol, flat screw

A pairwise Wilcoxon rank sum tests show that while the difference in roughness between the unused screws and any of the used screws is statistically significant, no significant differences are found between the screws from the various installation protocols (Table 23).

Table 22: Mean average roughness Ra (as measured, microns), flat screw

protocol	mean Ra
T	0.282 ± 0.104
TLT	0.279 ± 0.117
TT	0.267 ± 0.100
UNUSED	0.092 ± 0.012

Table 23: Pairwise Wilcoxon rank sum test p values (with Holm correction for multiple comparisons): average roughness (Ra), flat screw

	UNUSED	T	TT
T	0.014		
TT	0.014	1.000	
TLT	0.013	1.000	1.000

15 Scanning Electron Microscopy Results

Scanning electron microscopy (SEM) was employed in an attempt to qualitatively characterize the changes to the contact surfaces of the screw and simulated abutment counterbore that take place under each of the various installation protocols, and to draw qualitative comparisons between installation protocols. Only parts from the flat screw were included in the SEM analysis.

SEM images of the under-head seating surface of the screw, and the corresponding surface of the simulated abutment counterbore are presented here.

Figure 28 shows an unused 5979 screw. Parallel, regularly spaced circumferential striations are evident on all surfaces of the screw, which is characteristic of the turning operation used to manufacture the screws. A few light spots are visible on the seating surface, likely foreign matter debris.

Figure 29 shows a 5979 screw subjected to the T protocol. Some small (longest dimension <50 micron) lamellar structures are visible on the seating surface of the screw head. These lamellae seem to be attached to the surface of the screw. The long axes of these lamellae are generally oriented in a circumferential direction.

Figure 30 shows a 5979 screw subjected to the TT protocol. As in Figure 29, lamellae are visible on the seating surface of the screw. Compared with the screw shown in Figure 29, the number and concentration of the lamellae appear to be higher, to the point where multiple lamellae form a nearly continuous ring around the outer perimeter of the screw seating surface.

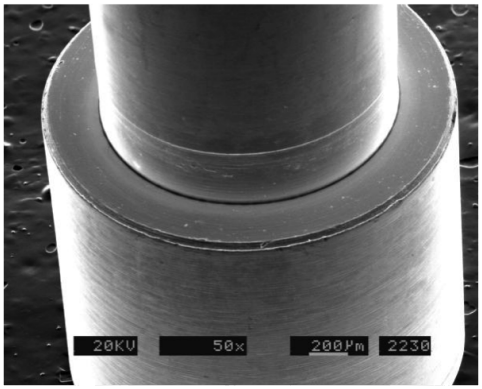

(a) 50x

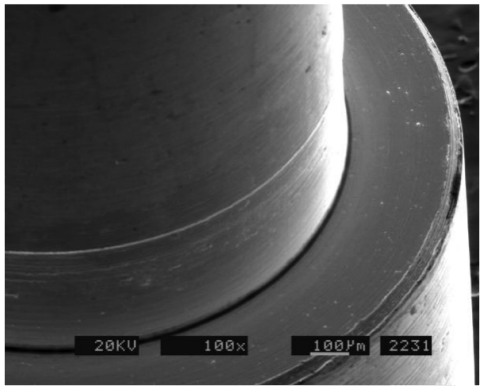

(b) 100x

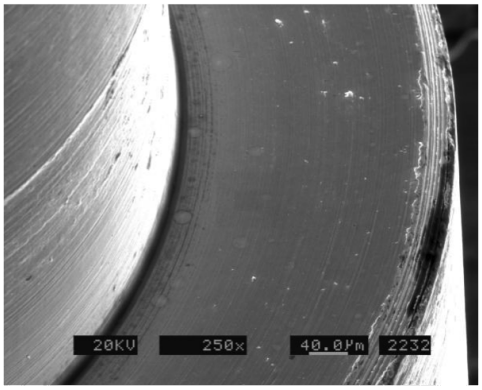

(c) 250x

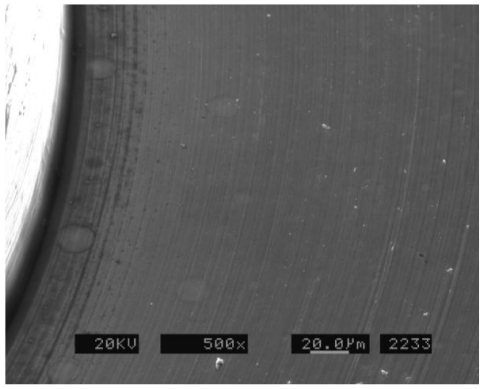

(d) 500x

Figure 28: SEM images, unused screw head seating surface

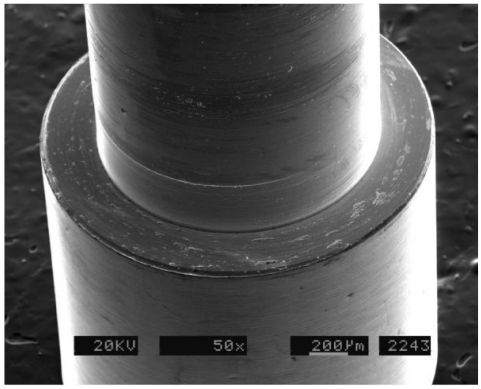

(a) 50x

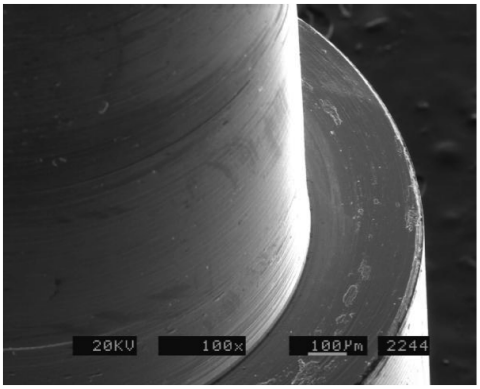

(b) 100x

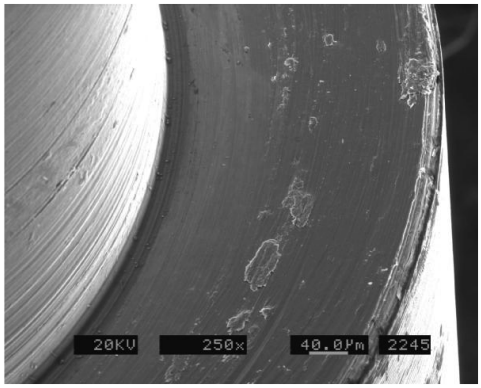

(c) 250x

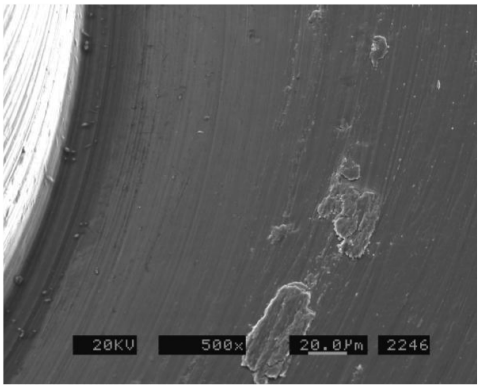

(d) 500x

Figure 29: SEM images, screw head seating surface, T protocol

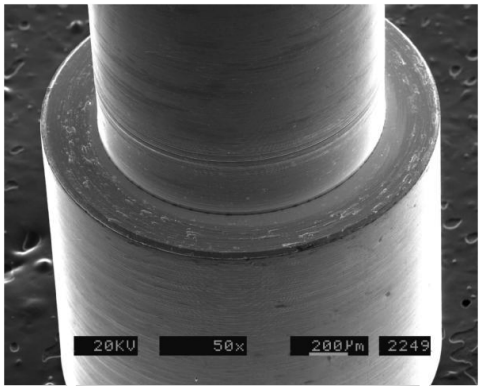

(a) 50x

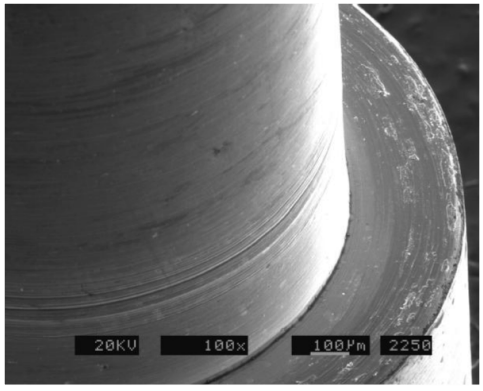

(b) 100x

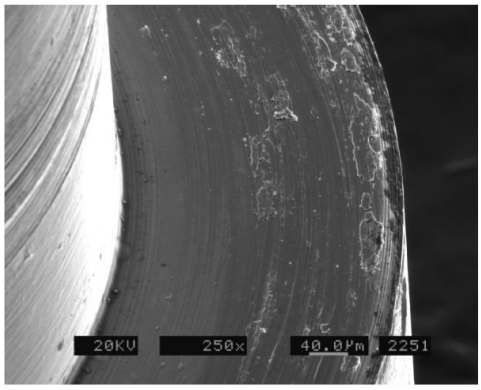

(c) 250x

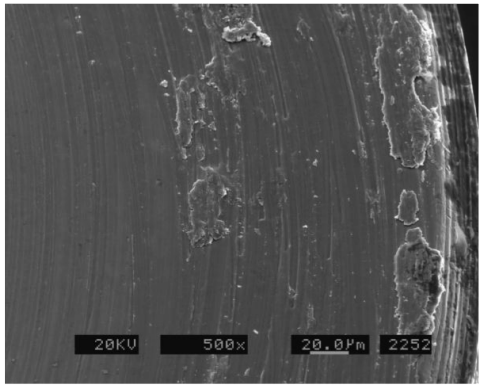

(d) 500x

Figure 30: SEM images, screw head seating surface, TT protocol

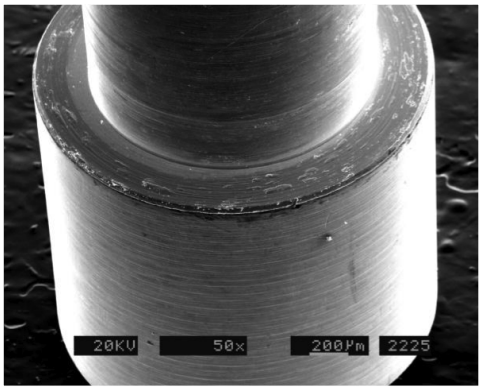

(a) 50x

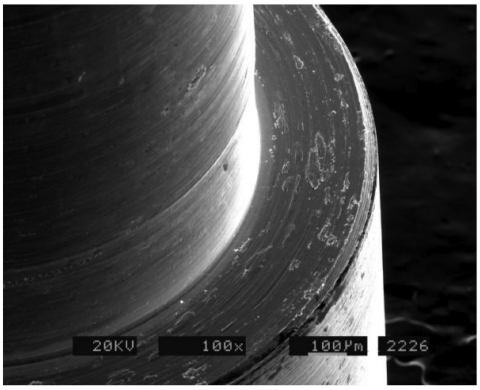

(b) 100x

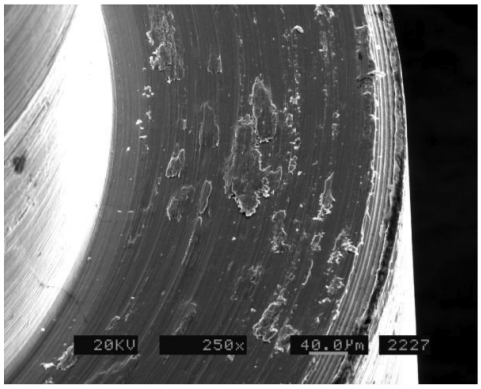

(c) 250x

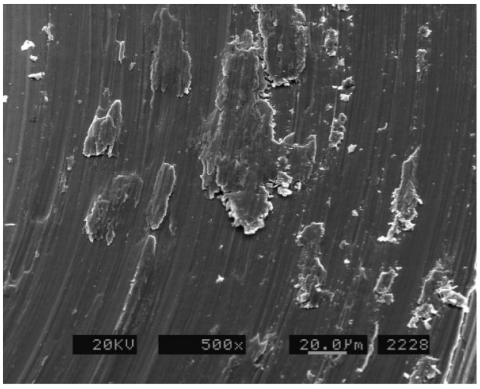

(d) 500x

Figure 31: SEM images, screw head seating surface, TLT protocol

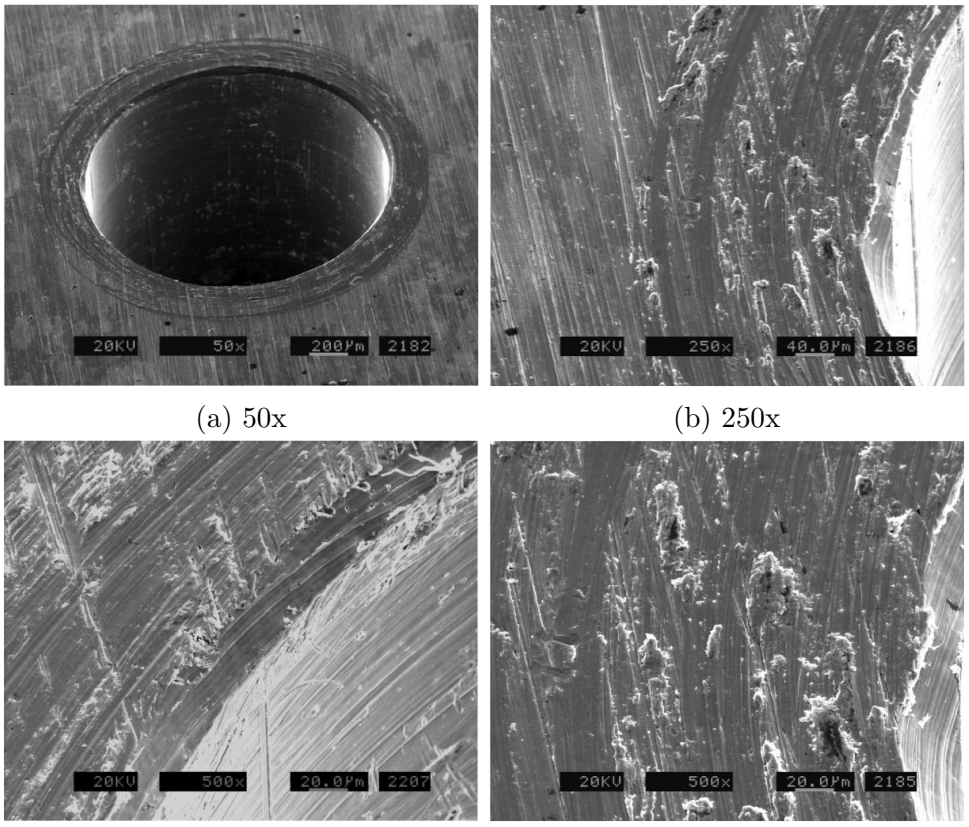

(a) 50x (b) 250x

(c) 500x (d) 500x

Figure 32: SEM images, counterbore seating surface, T protocol

Figure 31 shows a 5979 screw subjected to the TLT protocol. As in Figures 29 and 30, lamellae are visible on the seating surface of the screw. Compared with Figures 29 and 30, the number and concentration of the lamellae appear to be higher. The lamellae are dispersed over the entire seating surface of the screw, from the outer diameter of the screw head to the screw shank. Figures 31c and 31d show some circumferential depressions in the surface of the screw that may be evidence of material removal from the screw.

Figure 32 shows the simulated abutment counterbore surface for a 5979 screw subjected to the T protocol. Evident in Figure 32a are two distinct regions: the region immediately adjacent to the thru-bore, where the screw head made contact, is characterized by parallel, circumferential striations and small particles that appear adhered to the surface; and the region outside of

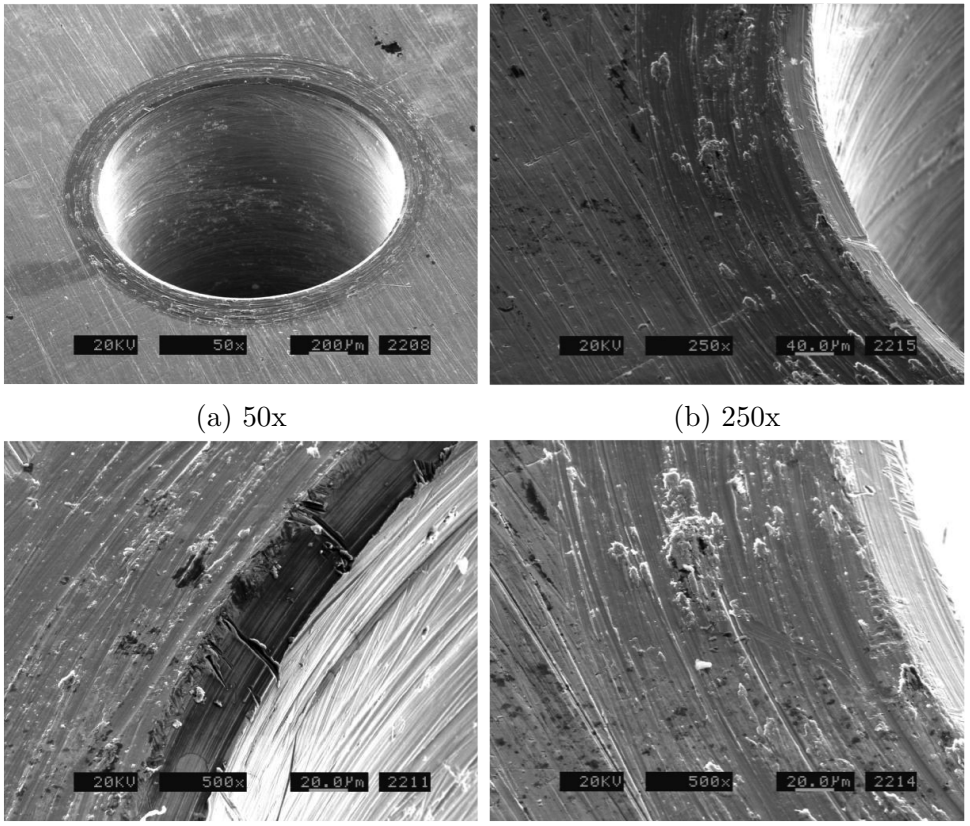

(a) 50x (b) 250x

(c) 500x (d) 500x

Figure 33: SEM images, counterbore seating surface, TT protocol

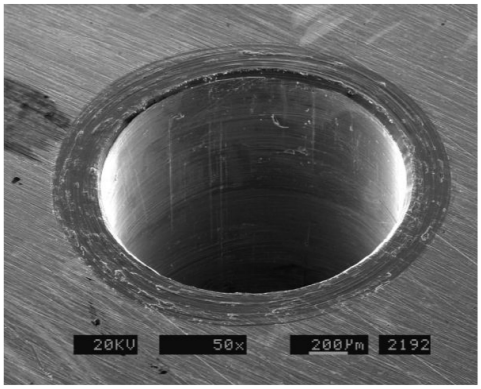

(a) 50x

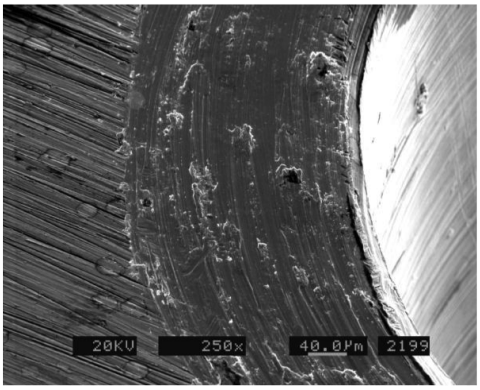

(b) 250x

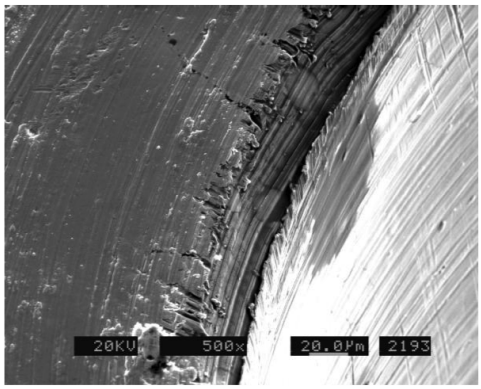

(c) 500x

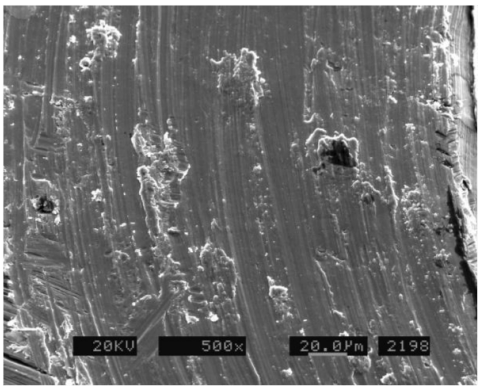

(d) 500x

Figure 34: SEM images, counterbore seating surface, TLT protocol

the area of contact with the screw, characterized by parallel, linear striations typical of a grinding manufacturing process. No adhered particles are visible outside of the area of contact with the screw head. Figure 32a shows linear machining marks continuing through the area of contact with the screw in the 5–11 o'clock region, with very little removal of the linear machining marks around 6–8 o'clock. These linear marks are also apparent continuing through the region of contact in Figures 32b, 32c, and 32d. The adhered wear particles evident in Figure 32 appear to be oriented with their long axis in a circumferential direction, and they appear to have negligible thickness on their counterclockwise-most edge, building to some maximum thickness near their clockwise-most edge (see Figures 32b and 32d).

Figure 33 shows the simulated abutment counterbore surface for a 5979 screw subjected to the TT protocol. Visually, the images are similar to those from the T protocol part shown in Figure 32, with some notable differences. Figure 33, from the TT protocol, shows complete obliteration of the linear grinding marks over a large portion of the region of contact with the screw head, with only the 3–6 o'clock region of Figure 33a showing some grinding marks remaining, particularly towards the outer diameter of the screw head. In comparison, Figure 32 from the T protocol shows grinding marks remaining over a much larger portion of the contact area. In addition, the circumferential striations in Figure 33 appear deeper than those in Figure 32.

Figure 34 shows the simulated abutment counterbore surface for a 5979 screw subjected to the TLT protocol. Figure 34a shows more thorough removal of linear machining marks inside the region of contact with the screw head than either Figure 32a or Figure 33a, though near the 6 o'clock position of Figure 34a, one particularly deep linear scratch remains visible.

16 White Light Interferometry Results

As a compliment to the SEM images, white light interferometry was employed in an attempt to help quantify the changes taking place on the contact surfaces of the abutment screw and simulated abutment counterbore.

A white light interferometry image of a screw and the matching counterbore for the T protocol is shown in Figure 35. A screw and the matching counterbore for the TT protocol is shown in Figure 36. A screw and the matching counterbore for the TLT protocol is shown in Figure 37.

Based on the color scale, it appears that the lamellar structures evident in the SEM images are approximately 3–8 microns thick, and are generally smooth on their surface.

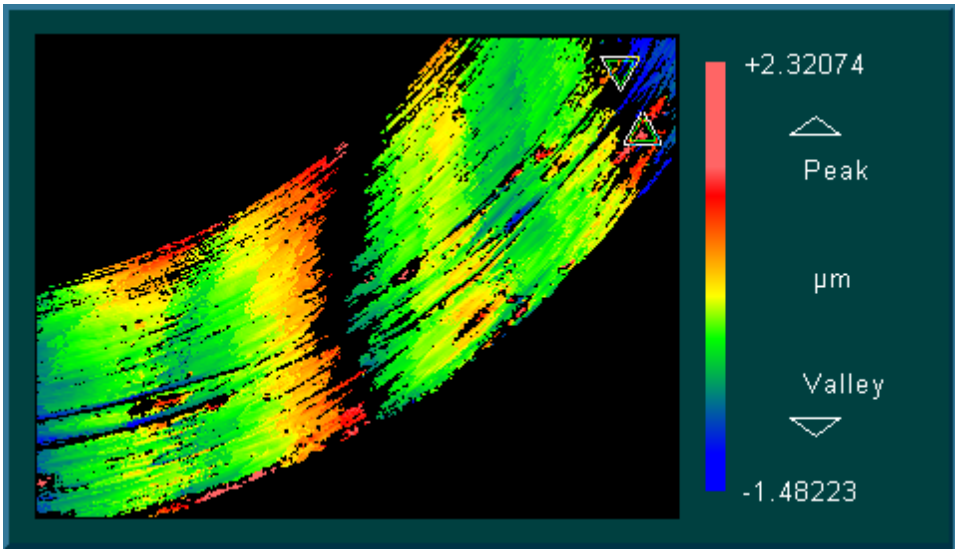

(a) Screw

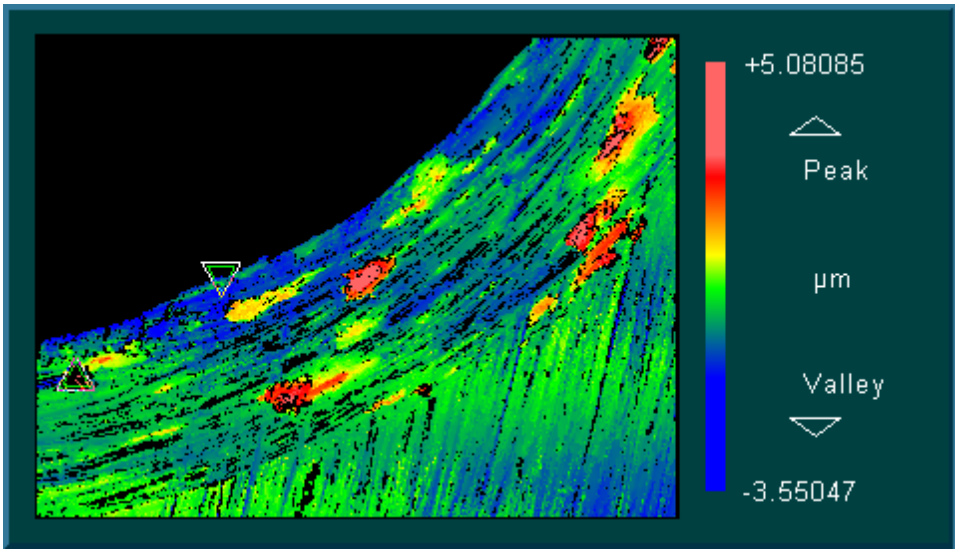

(b) Counterbore

Figure 35: White light interferometry images, 5979 screw, T protocol

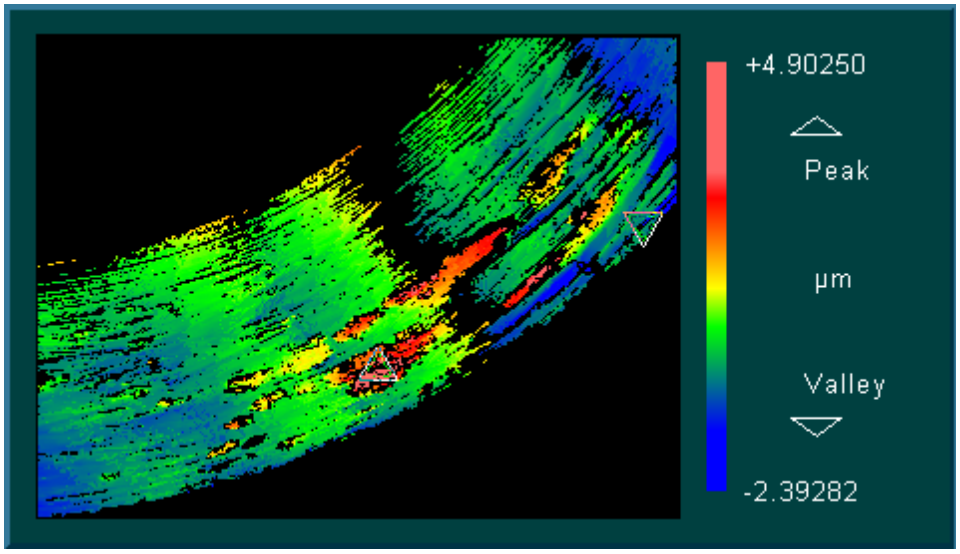

(a) Screw

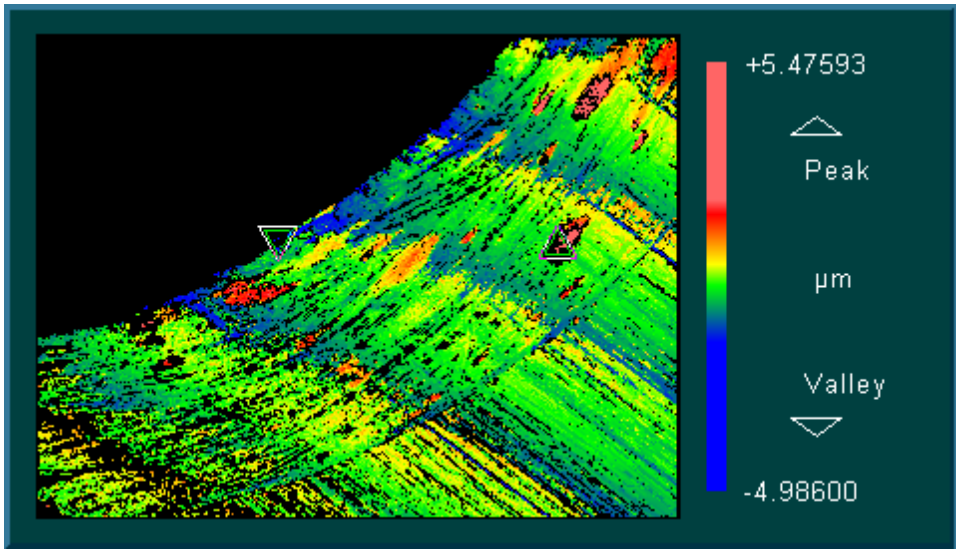

(b) Counterbore

Figure 36: White light interferometry images, 5979 screw, TT protocol

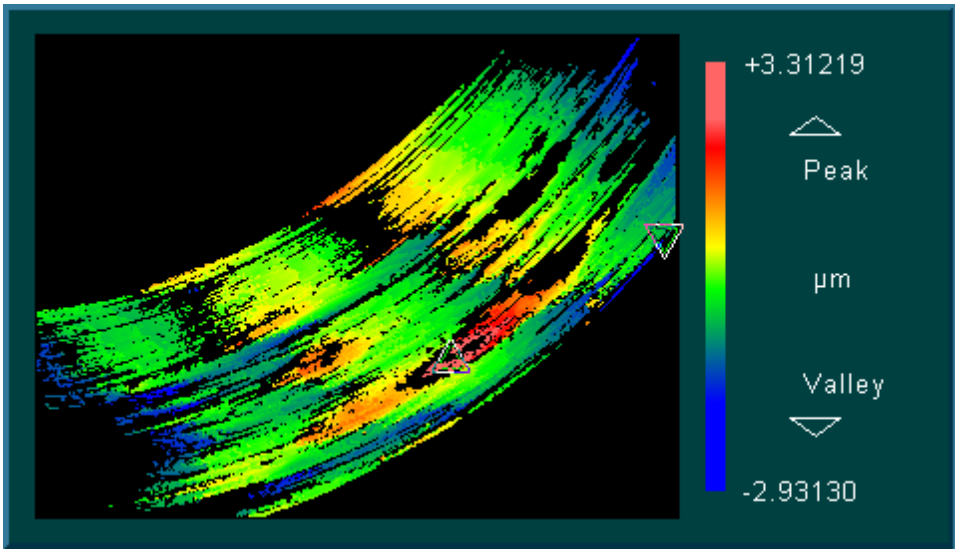

(a) Screw

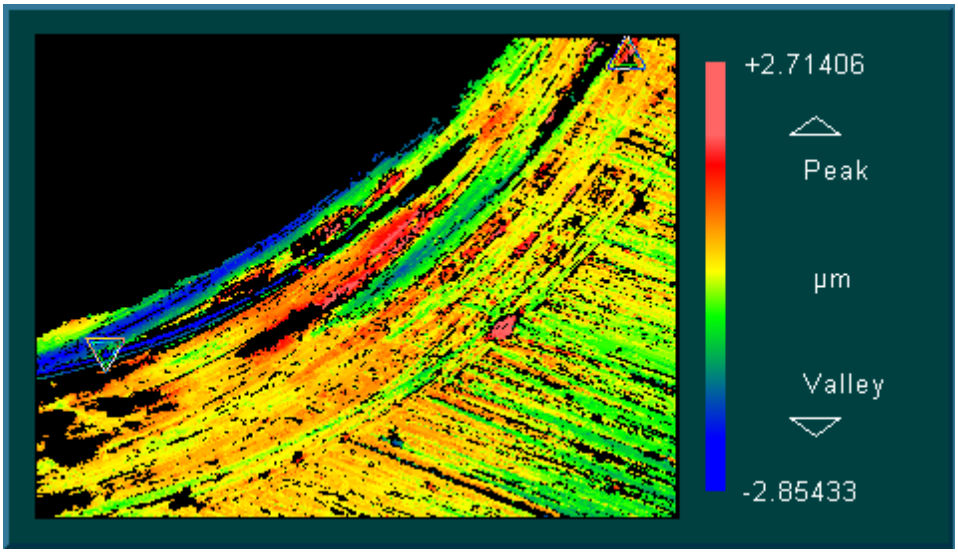

(b) Counterbore

Figure 37: White light interferometry images, 5979 screw, TLT protocol

17 Discussion

17.1 Screw Stiffness

The relationship between screw elongation and preload in the joint is a simple one; the screw is effectively a stiff spring. The elongation of the screw can be estimated based on geometry, material properties, and load:

$$\Delta_L = \frac{F_P}{E}\left(\frac{L_b + L_h/2}{A_b} + \frac{L_t + L_e/2}{A_t}\right) \tag{17.1}$$

The mechanism that is believed to be responsible for the loss of preload observed in this study is embedment relaxation, where surface asperities at the contact areas of the joint are crushed, leading to a decrease in the elongation of the screw, which results in a loss of preload. In a screw with low stiffness, a given decrease in elongation results in a small drop in preload; in a screw with higher stiffness, the same decrease in elongation results in a larger drop in preload. On this basis, a screw with low stiffness should be less susceptible to preload loss from embedment relaxation than a screw with high stiffness.

The pilot study conducted as part of this effort yielded a low absolute preload loss with high variability between replicates. In an attempt to increase the statistical power of the main study, screws that were shorter than those used in the pilot study, and therefore stiffer, were selected for the main study.

The screw stiffness can be estimated by re-arranging Equation 17.1:

$$K = \frac{F_P}{\Delta L} = E\left(\frac{A_b}{L_b + L_h/2} + \frac{A_t}{L_t + L_e/2}\right) \tag{17.2}$$

Table 24 includes stiffness estimates derived from Equation 17.2. Based on these estimates, the flat screw used in the main study is 34% stiffer than the screw used in the pilot study. It was expected that the amount of embedment

relaxation, measured as a linear dimension, would be roughly the same between the pilot study and the main study, and therefore the stiffer screw used in the main study would show an increase in preload loss of similar magnitude to the increase in screw stiffness.

In fact, by back-calculating the estimated relaxation for the pilot study and the main study using the observed preload loss and Equation 17.1, less linear relaxation was observed in the main study than the pilot study (0.18 µm vs. 0.32 µm, see Table 24).

Table 24: Screw stiffness and relaxation, flat screws, pilot and main study

	Pilot Study	Main Study
l_h (mm)	2.00	1.80
d_h (mm)	2.35	2.15
l_b (mm)	4.70	1.56
d_b (mm)	1.60	1.56
l_t (mm)	1.25	2.04
d_t (mm)	1.27	1.27
l_e (mm)	2.40	2.40
E (GPa)	110	110
Est. Stiffness, k (N/µm)	96	129
Mean Preload Loss, T protocol, 12 hours (N)	7.4	8.8
Est. Mean Relaxation (µm)	0.32	0.18

This somewhat unexpected outcome could be due to differences in surface condition of the fixturing, as the simulated implants and counterbores were sourced from a different supplier for the main study than the pilot study. Another potential explanation can be found in the change from cut threads to rolled threads on the abutment screw between the pilot study and the main study. The rolled threads of the flat screw in the main study have undergone cold-working in the manufacturing process, which likely yields a harder surface on the screw threads, which may be less susceptible to embedment relaxation.

17.2 Tapered vs. Flat Screws

Both initial and residual preload were higher for the flat screw than the tapered screw. This result is expected, as the tapered screw head creates a wedging effect against the tapered counterbore, which results in higher frictional reaction torque at the screw head as compared with the flat screw. As a result, less of the installation torque is available to stretch the screw and create preload in the tapered screw.

Across all installation protocols, the relative preload loss for the screw with the tapered seating surface was greater than for the screw with the flat seating surface. This is consistent with the mechanism of embedment relaxation [2].

Flattening of asperities at the seating surface of the screw happens normal to the seating surface, and preload loss results when the screw relaxes along its long axis. If the seating surface is inclined relative to the long axis of the screw, the axial relaxation of the screw is amplified by a factor equal to $\frac{1}{\sin\phi}$, where ϕ is the half angle of the taper [2].

In the case of the tapered screw, $\phi = 41^\circ$, so the geometric amplification factor can be calculated as

$$\frac{1}{\sin 41^\circ} \approx 1.52$$

Experimentally, within the T group, which can be viewed as the control, the mean preload loss at 120 min was 3.4% for the tapered screw, and 2.0% for the flat screw (Table 16).

The ratio of observed preload loss within the T group for the tapered 5764 screw relative to the flat 5979 screw is 1.66. This is a mere 9% error relative to the above theoretical calculation. This can be viewed as evidence in support of the theory that some preload loss occurs due to embedment relaxation.

It should also be noted that the flat screw has rolled threads, while the

tapered screw has cut threads. This difference in manufacturing approach could have some potentially confounding effects on the comparative results between the flat and tapered screw, as the surface texture of the threads may be different, and the hardness of the screw threads may be different due to the cold-working that takes place during thread rolling. This cold working would tend to make the rolled threads harder, which may decrease the amount of embedment relaxation taking place at the rolled threads. This may account for some of the difference between the theoretical and experimental amplification factor. Any difference in friction coefficient between the cut and rolled threads could affect the observed difference in initial and residual preload between the flat screw with rolled threads and the tapered screw with cut threads.

17.3 Magnitude of Relative Preload Loss

Cantwell and Hobkirk conducted a study examining preload loss in gold alloy prosthetic retaining screws (small screws used to attach a final restoration, such as an implant supported framework, to a standard abutment), and their study found a mean preload loss of 24.9% after 15 hours, with 40.2% of this loss occurring within 10 seconds of tightening [5].

The present study found far less relative preload loss (an average of 2.3% after 12 hours for the flat screw without retightening). This difference is likely due to the difference between the components tested by Cantwell and Hobkirk and those used in this study. The Cantwell and Hobkirk study used gold prosthetic cylinders and gold prosthetic retaining screws. These gold components have a significantly lower yield strength than do the titanium components used in the present study, therefore the gold components are more susceptible to embedment relaxation than the titanium components. The Cantwell and Hobkirk study also used a hand-made load transducer formed by applying

three strain gauges to an implant abutment, as compared to the commercial strain gauge of the present study.

It should also be noted that an actual implant/screw/abutment assembly can experience additional embedment relaxation at the implant/abutment interface, while the fixture used in the present study, by virtue of its much-larger area of contact between components, is not likely to experience any significant embedment effects other than those directly related to contact between the screw and its mating elements. As a result, it may be reasonable to expect more embedment relaxation, and thus more preload loss, to occur in an actual implant/abutment/screw assembly than was observed in this study.

17.4 Effect of Installation Protocol on Relative Preload Loss

The T group had a higher relative preload loss than either the TT or the TLT group, demonstrating that either of the retightening procedures can impact the relative load loss that occurs after retightening.

The effect is more pronounced with the 5764 screw, which has a tapered seating surface, than with the 5979 screw, which has a flat seating surface.

The TT protocol showed less relative preload loss than the TLT protocol. This is likely due to the way that relative preload loss was defined for this study, and how that relates to the typical time signature of the preload loss. Much of the preload loss happens immediately upon completion of tightening. It may be that the TT protocol, which involves a mere re-application of the initial tightening torque, does not fully re-start this time signature, and so following the re-tightening, the joint in the TT protocol is following an "abridged" preload loss curve. The TLT protocol, in contrast, is completely loosened and re-tightened, so following re-tightening, the joint again follows the full preload

loss curve, albeit a less severe one than the T protocol as evidenced by the relative load loss results.

Relative preload loss as defined in this study is an interesting quantity because it reflects what happens to the preload in the joint after the last tightening event. It should be noted, however, that the quantity that is arguably more important from a clinical perspective is the residual preload, i.e. the preload left in the joint at the conclusion of the observation period.

17.5 Effect of Installation Protocol on Residual Preload

The effect of the installation protocol on the level of residual preload was not nearly as clear as its effect on the level of relative preload loss. The Kruskal-Wallis test showed that installation protocol had an effect on the level of residual preload for the tapered screw, but not for the flat screw.

For the 5764 screw, with a tapered seating surface, the TLT protocol produced a mean residual preload higher than both the T protocol and the TT protocol; a noteworthy result, and one that confirms the hypothesis that the sequence in which torque is applied to an abutment screw, such as to tighten and retighten, or to tighten followed by loosening and retightening, has a significant effect on the immediate degradation of screw preload prior to the application of external loading.

Surface characterization by SEM, Interferometry, and profilometry were not carried out on the parts with a tapered seating surface, due to the additional difficulty that the taper would impose upon those methods, so one can only speculate on the exact mechanism that explains the increased residual preload for the TLT protocol on the tapered screw.

While the TLT protocol failed to produce a significant difference in mean residual protocol for the flat-headed 5979 screw, the TLT protocol did produce

significantly reduced residual preload variance for the flat screw (Figure 24, Table 15). The range of residual preload for the flat screw with the T protocol was 325.0–401.6 N, compared with 355.6–386.5 N, for the TLT protocol. The TLT protocol cut the range of residual preload more than in half compared to the T protocol. This is not without clinical significance on its own, as securing more predictable outcomes for patients is clearly an important goal of dentistry.

The finding that retightening protocols demonstrated a significant reduction in residual preload variance may in fact be the most important finding of this study. Some theories of screw loosening hold that once preload falls below some critical level, self-loosening can occur, whereby the screw begins turning in the joint under conditions of vibration or cyclic loading [2]. If this is indeed the case, then the "low preload outliers" that are evident in the T group may be the most susceptible to self-loosening or other failure. The retightening protocols tested in this study resulted in significant reductions in preload variance, and fewer outliers are evident in the TT and TLT groups. This makes a compelling argument in favor of retightening protocols.

17.6 Effect of Installation Protocol on Initial Preload

For the purposes of this study, we define initial preload as the preload in the joint immediately upon completion of the final tightening intervention.

Given that the peak installation torque was held constant throughout the study, the initial preload is fundamentally a function of the effective friction between the screw and the joint members at the threads and the under-head seating surface.

The results for initial preload are perhaps some of the most interesting in the study. For the 5764 screw, with a tapered seating surface, we see that

the TLT protocol produces significantly higher initial preload than both the T protocol and the TT protocol (Tables 8 and 9); yet for the 5979 screw, with a flat seating surface, we find that the TLT protocol produced significantly *lower* initial preload than the T protocol (Tables 8 and 10). While the magnitude of the effect is not large in either case, it is curious that the direction of the effect is opposite for the two screw geometries.

Lacking any images or measurements to directly evaluate the effects of installation protocol on the contact surfaces of the tapered screw, it is difficult to say what the cause of this strange opposite-direction effect is, though one possibility is that a slight angular mis-fit between the tapered screw head and the tapered counterbore of the as-machined, unused parts causes some binding when the parts are first tightened, resulting in high underhead friction for the first installation, while on the second installation this binding has been reduced by plastic deformation (bedding-in) of the contact surfaces.

17.7 Roughness Measurement

The roughness measurements conducted using the profilometer did not indicate a correlation between surface roughness and installation protocol or preload loss. For all of the used parts the Ra measurements were dominated by the waviness component (Wa), which was likely introduced by tracing over the large adhered wear particles that are visible in the SEM and interferometry images.

17.8 SEM Images

As is often the case, you can tell a lot by looking at something. In this case, one of the best tools for looking at these screws and simulated abutment counterbores is certainly an SEM. The unused screw is clearly pristine (Figure 28),

while each of the used screws contain what appear to be adhered wear particles (Figures 29, 30 and 31).

The adhered wear particles visible on the screws seem to each have clearly defined boundaries, as if they were applied to the screw surface, rather than born out of the screw surface. This is in contrast to the adhered wear particles visible in the SEM pictures of the counterbore seating surface (Figures 32, 33 and 34), where the clockwise-most edge of many of the wear particles appears clearly defined, while the counterclockwise-most edge of the wear particle is absent. This suggests that these wear particles were smeared or plowed out of the surface of the simulated counterbore.

The abutment screw and simulated abutment counterbore are made of the same material (Ti 6Al-4V ASTM F-136 ELI), and so should have similar material properties. It is therefore interesting that the simulated abutment counterbore seems to have suffered the brunt of the surface wear. This could be due to the difference in starting surface finish on the two parts, or difference in the degree of cold working during the fabrication process.

Comparing the turned surface of the unused screw shown in Figure 28c to a similar-magnification image of the ground surface of the simulated abutment counterbore visible at the left of Figure 34b, the as-machined surface of the simulated counterbore certainly seems rougher than the as-machined surface of the screw head. It could be then that as the screw is tightened against the simulated counterbore, the peaks of the as-ground surface of the counterbore are worn down and smeared out, while the comparatively flatter surface of the screw head suffers little wear.

Progressing through the images of the screws from the T protocol to the TT protocol to the TLT protocol, the quantity of adhered wear particles seems to increase (Figures 29, 30 and 31). This could be a cause for increased friction

between the screw head and the simulated abutment counterbore, a possible explanation for the observed decreased initial preload of the TLT protocol as compared to the T protocol.

Progressing through the images of the simulated abutment counterbores from the T protocol to the TT protocol to the TLT protocol, the portion of the contact region over which all of the initial machining marks are obliterated seems to increase (Figures 32, 33 and 34). It would seem that the machining marks are more thoroughly worn down in the part from the TLT protocol than the part from the TT protocol, which is in turn more thoroughly worn down than the part from the T protocol.

It may be that the ground surface of the simulated abutment counterbore for the flat screw does not accurately reflect the types of surfaces that would be seen in actual titanium abutments. In fact, it is exceedingly unlikely, if not impossible, that the counterbore surface of an abutment would be machined in such a way as to leave parallel, linear machining marks. Therefore caution should be observed when extending the results of the study for the flat screw to actual abutments. The simulated counterbore for the tapered screw, however, probably more accurately represents the type of surface that one would expect in an abutment for a tapered abutment screw, as the drilling process used to create the simulated counterbore is likely very similar to what would be used to produce an actual abutment.

17.9 Interferometry Images

The interferometry images tell a similar story to the SEM images. The interferometry images, while lower-resolution than the SEM images, have the benefit including quantified surface topography measurements. This color scale shows that the lamellar structures observed in the SEM images are relatively smooth

on their surface. In some cases, the lamellae can be seen to be building in thickness from their leading to trailing edge (based on the direction of tightening).

18 Conclusions

Re-torquing protocols (tighten, then retighten 10 minutes later, the TT protocol; or tighten, then 10 minutes later loosen and retighten, the TLT protocol) should be considered as a means to decrease relative preload loss, increase residual preload, and decrease variability in residual preload in dental implant/abutment screw joints.

- The TT protocol produced the lowest relative preload loss for both the tapered abutment screw and the flat abutment screw
- The TLT protocol produced higher residual preload for the tapered abutment screw than both the T protocol and the TT protocol
- The various re-torquing protocols produced no statistically significant difference in residual preload for the flat abutment screw
- The TLT protocol significantly reduced the variance in residual preload for the flat abutment screw compared with both the T protocol and the TT protocol
- Scanning electron microscopy (SEM) images showed adhesive wear patches on the contact surfaces of the flat screw, indicating that some break-in of contact surfaces does take place during tightening, and the quantity of these wear patches was seen to be higher for the TT protocol and the TLT protocol.

19 Future Work

The present study had certain methodological limitations, and exposed certain new areas for study. Future work may be warranted along the following lines:

- Repeat the study using actual (suitably modified) implants and abutments
- Perform a similar study to evaluate the effectiveness of coated abutment screws (gold coated, diamond-like-carbon coated)
- Repeat the study in a lubricated environment (simulating the oral environment)
- Evaluate the effect of repeated loosening and retightening

Works Cited

[1] M. Al Rafee, W. Nagy, and R. Fournelle, "The effect of repeated torque on the ultimate tensile strength of slotted gold prosthetic screws," *The Journal of prosthetic dentistry*, 2002.

[2] J. H. Bickford, *An Introduction to the Design and Behavior of Bolted Joints*. Taylor & Francis Group, 1995.

[3] L. C. Breeding, D. L. Dixon, E. W. Nelson, and J. D. Tietge, "Torque required to loosen single-tooth implant abutment screws before and after simulated function.," *The International journal of prosthodontics*, 1993.

[4] D. Byrne, S. Jacobs, B. O'Connell, F. Houston, and N. Claffey, "Preloads Generated with Repeated Tightening in Three Types of Screws Used in Dental Implant Assemblies," *Journal of Prosthodontics*, 2006.

[5] A. Cantwell and J. A. Hobkirk, "Preload loss in gold prosthesis-retaining screws as a function of time.," *The International journal of oral & maxillofacial implants*, 2004.

[6] K. L. Goheen, S. G. Vermilyea, J. Vossoughi, and J. R. Agar, "Torque generated by handheld screwdrivers and mechanical torquing devices for osseointegrated implants.," *The International journal of oral & maxillofacial implants*, 1994.

[7] T. Guda, T. Ross, L. Lang, and H. Millwater, "Probabilistic analysis of preload in the abutment screw of a dental implant complex," *The Journal of prosthetic dentistry*, 2008.

[8] S. Holm, "A simple sequentially rejective multiple test procedure," *Scandinavian journal of statistics*, 1979.

[9] R. E. Jung, B. E. Pjetursson, R. Glauser, A. Zembic, M. Zwahlen, and N. P. Lang, "A systematic review of the 5-year survival and complication rates of implant-supported single crowns," *Clinical Oral Implants Research*, 2008.

[10] A. Kanawati, M. W. Richards, J. J. Becker, and N. E. Monaco, "Measurement of clinicians' ability to hand torque dental implant components.," *The Journal of oral implantology*, 2009.

[11] G. Krennmair, R. Seemann, A. Fazekas, R. Ewers, and E. Piehslinger, "Patient preference and satisfaction with implant-supported mandibular overdentures retained with ball or locator attachments: a crossover clinical trial.," *The International journal of oral & maxillofacial implants*, 2012.

[12] "North American Markets for Dental Implants 2010," Millenium Research Group, Tech. Rep., 2010.

[13] *R: A Language and Environment for Statistical Computing*.

[14] T. J. Salinas, M. S. Block, and A. Sadan, "Fixed partial denture or single-tooth implant restoration? Statistical considerations for sequencing and treatment," *Journal of Oral and Maxillofacial Surgery*, 2004.

[15] G. Siamos and S. Winkler, "The Relationship Between Implant Preload and Screw Loosening on Implant-supported Prostheses," *Journal of Oral Implantology*, 2002.

[16] M. Torabinejad, P. Anderson, J. Bader, L. J. Brown, L. H. Chen, C. J. Goodacre, M. T. Kattadiyil, D. Kutsenko, J. Lozada, R. Patel, F. Petersen, I. Puterman, and S. N. White, "Outcomes of root canal treatment and restoration, implant-supported single crowns, fixed partial dentures, and extraction without replacement: A systematic review," *The Journal of prosthetic dentistry*, 2007.

[17] G. K. Tzenakis, W. W. Nagy, R. A. Fournelle, and V. B. Dhuru, "The effect of repeated torque and salivary contamination on the preload of slotted gold implant prosthetic screws.," *The Journal of prosthetic dentistry*, 2002.

[18] M. C. Vallee, H. J. Conrad, S. Basu, and W.-J. Seong, "Accuracy of friction-style and spring-style mechanical torque limiting devices for dental implants.," *The Journal of prosthetic dentistry*, 2008.

[19] R. Vogel, J. Smith-Palmer, and W. Valentine, "Evaluating the health economic implications and cost-effectiveness of dental implants: a literature review.," *The International journal of oral & maxillofacial implants*, 2013.

[20] F. Zarone, R. Sorrentino, T. Traini, D. Di lorio, and S. Caputi, "Fracture resistance of implant-supported screw- versus cement-retained porcelain fused to metal single crowns: SEM fractographic analysis," *Dental Materials*, 2007.

Further Reading

[21] N. D. Adatia, S. C. Bayne, L. F. Cooper, and J. Y. Thompson, "Fracture Resistance of Yttria-Stabilized Zirconia Dental Implant Abutments," *Journal of Prosthodontics*, 2009.

[22] Y. S. Al Jabbari, R. Fournelle, G. Ziebert, J. Toth, and A. Iacopino, "Mechanical behavior and failure analysis of prosthetic retaining screws after long-term use in vivo. Part 2: Metallurgical and microhardness analysis.," *Journal of Prosthodontics*, 2008.

[23] Y. S. Al Jabbari, R. Fournelle, G. Ziebert, J. Toth, and A. M. Iacopino, "Mechanical Behavior and Failure Analysis of Prosthetic Retaining Screws after Long-term Use In Vivo. Part 1: Characterization of Adhesive Wear and Structure of Retaining Screws," *Journal of Prosthodontics*, 2008.

[24] ——, "Mechanical Behavior and Failure Analysis of Prosthetic Retaining Screws after Long-term Use In Vivo. Part 3: Preload and Tensile Fracture Load Testing," *Journal of Prosthodontics*, 2008.

[25] ——, "Mechanical Behavior and Failure Analysis of Prosthetic Retaining Screws after Long-term Use in vivo. Part 4: Failure Analysis of 10 Fractured Retaining Screws Retrieved from Three Patients," *Journal of Prosthodontics*, 2008.

[26] I. Alkan and A. Sertgöz, "Influence of occlusal forces on stress distribution in preloaded dental implant screws," *The Journal of prosthetic dentistry*, 2004.

[27] P. P. Binon and M. J. McHugh, "The effect of eliminating implant/abutment rotational misfit on screw joint stability.," *The International journal of prosthodontics*, 1996.

[28] D. Bozkaya and S. Müftü, "Mechanics of the taper integrated screwed-in (TIS) abutments used in dental implants," *Journal of Biomechanics*, 2005.

[29] R. BURGUETE, R. JOHNS, T. KING, and E. PATTERSON, "Tightening characteristics for screwed joints in osseointegrated dental implants," *The Journal of prosthetic dentistry*, 1994.

[30] F. BUTZ, G. HEYDECKE, M. OKUTAN, and J. R. STRUB, "Survival rate, fracture strength and failure mode of ceramic implant abutments after chewing simulation," *Journal of Oral Rehabilitation*, 2005.

[31] M. Cardoso, M. F. Torres, E. J. V. Lourenço, D. de Moraes Telles, R. C. S. Rodrigues, and R. F. Ribeiro, "Torque removal evaluation of prosthetic screws after tightening and loosening cycles: an in vitro study," *Clinical Oral Implants Research*, 2011.

[32] A. Carr, J. Brunski, and E. Hurley, "Effects of fabrication, finishing, and polishing procedures on preload in prostheses using conventional "gold' and plastic cylinders.," *The International journal of oral & maxillofacial implants*, 1996.

[33] A. Carr, P. E. Larsen, E. Papazoglou, and E. McGlumphy, "Reverse torque failure of screw-shaped implants in baboons: baseline data for

abutment torque application.," *The International journal of oral & maxillofacial implants*, 1995.

[34] E. Cavazos and F. A. Bell, "Preventing loosening of implant abutment screws," *The Journal of prosthetic dentistry*, 1996.

[35] R. Cibirka, "Examination of the implant—abutment interface after fatigue testing," *The Journal of prosthetic dentistry*, 2001.

[36] C. J. Drago, "A clinical study of the efficacy of gold-tite square abutment screws in cement-retained implant restorations.," *The International journal of oral & maxillofacial implants*, 2003.

[37] C. Elias, D. Figueira, and P. Rios, "Influence of the coating material on the loosing of dental implant abutment screw joints," *Materials Science and Engineering: C*, 2006.

[38] P. Gehrke, G. Dhom, J. Brunner, and D. Wolf, "Zirconium implant abutments: fracture strength and influence of cyclic loading on retaining-screw loosening," *QUINTESSENCE ...*, 2006.

[39] D. Gratton, "Micromotion and dynamic fatigue properties of the dental implant–abutment interface," *The Journal of prosthetic dentistry*, 2001.

[40] J. E. Haack, R. L. Sakaguchi, T. Sun, and J. P. Coffey, "Elongation and preload stress in dental implant abutment screws.," *The International journal of oral & maxillofacial implants*, 1995.

[41] E. E. Hill, S. M. Phillips, and L. C. Breeding, "Implant abutment screw torque generated by general dentists using a hand driver in a limited access space simulating the mouth.," *The Journal of oral implantology*, 2007.

[42] S. Hoyer, "Dynamic fatigue properties of the dental implant–abutment interface: Joint opening in wide-diameter versus standard-diameter hex-type implants," *The Journal of prosthetic dentistry*, 2001.

[43] M. J. Jaarda, M. E. Razzoog, and D. G. Gratton, "Effect of preload torque on the ultimate tensile strength of implant prosthetic retaining screws.," *Implant dentistry*, 1994.

[44] T. Kallus and C. Bessing, "Loose gold screws frequently occur in full-arch fixed prostheses supported by osseointegrated implants after 5 years.," *The International journal of oral & maxillofacial implants*, 1994.

[45] A. Khraisat, "Effect of lateral cyclic loading on abutment screw loosening of an external hexagon implant system," *The Journal of prosthetic dentistry*, 2004.

[46] ——, "Fatigue resistance of two implant/abutment joint designs," *The Journal of prosthetic dentistry*, 2002.

[47] K.-S. Kim, Y.-J. Lim, M.-J. Kim, H.-B. Kwon, J.-H. Yang, J.-B. Lee, and S.-H. Yim, "Variation in the total lengths of abutment/implant assemblies generated with a function of applied tightening torque in external and internal implant-abutment connection," *Clinical Oral Implants Research*, 2010.

[48] T. Kitagawa, Y. Tanimoto, M. Odaki, K. Nemoto, and M. Aida, "Influence of implant/abutment joint designs on abutment screw loosening in a dental implant system," *Journal of Biomedical Materials Research Part B: Applied Biomaterials*, 2005.

[49] L. Lang, "Finite element analysis to determine implant preload," *The Journal of prosthetic dentistry*, 2003.

[50] M. Marlowe, "Elasticity and Internal Friction of Polycrystalline Yttrium Oxide - MARLOWE - 2006 - Journal of the American Ceramic Society - Wiley Online Library," *Journal of the American Ceramic ...*, 1965.

[51] W. Martin, "Implant abutment screw rotations and preloads for four different screw materials and surfaces," *The Journal of prosthetic dentistry*, 2001.

[52] E. A. McGlumphy, D. A. Mendel, and J. A. Holloway, "Implant screw mechanics.," *Dent. Clin. North Am.*, 1998.

[53] J. Nissan, M. Gross, A. Shifman, and D. Assif, "Stress levels for well-fitting implant superstructures as a function of tightening force levels, tightening sequence, and different operators.," *The Journal of prosthetic dentistry*, 2001.

[54] J.-K. Park, J.-U. Choi, Y.-C. Jeon, K.-S. Choi, and C.-M. Jeong, "Effects of abutment screw coating on implant preload," *Journal of Prosthodontics*, 2010.

[55] E. A. Patterson and R. B. Johns, "Theoretical analysis of the fatigue life of fixture screws in osseointegrated dental implants.," *The International journal of oral & maxillofacial implants*, 1992.

[56] T. Sadowski, "Modeling of Porous Ceramics Response to Compressive Loading - Sadowski - 2004 - Journal of the American Ceramic Society - Wiley Online Library," *Journal of the American Ceramic ...*, 2003.

[57] R. L. Sakaguchi and S. E. Borgersen, "Nonlinear contact analysis of preload in dental implant screws.," *The International journal of oral & maxillofacial implants*, 1995.

[58] S. Scheuber, S. Hicklin, and U. Brägger, "Implants versus short-span fixed bridges: survival, complications, patients' benefits. A systematic review on economic aspects," *Clinical Oral Implants Research*, 2012.

[59] M. S. Schwarz, "Mechanical complications of dental implants," *Clinical Oral Implants Research*, 2000.

[60] J. E. Shigley, C. R. Mischke, and R. G. Budynas, *Mechanical Engineering Design*. McGraw Hill, 2004.

[61] R. Stüker, E. Teixeira, J. Beck, and N. Da Costa, "Preload and torque removal evaluation of three different abutment screws for single standing implant restorations," *Journal of Applied Oral Science*, 2008.

[62] J. K. Sutherland, R. G. Ritsco, and S. R. Budd, "Marginal Adaptation of Implant-Supported Metal-Ceramic Crowns Fabricated With Gold Cylinders," *Journal of Prosthodontics*, 1998.

[63] K. Tan and J. Nicholls, "Implant-abutment screw joint preload of 7 hex-top abutment systems.," *The International journal of oral & maxillofacial implants*, 2001.

[64] A. Theoharidou, H. Petridis, K. Tzannas, and P. Garefis, "Abutment screw loosening in single-implant restorations: A systematic review," *The International journal of oral & maxillofacial implants*, 2008.

[65] T. Tsuge and Y. Hagiwara, "Influence of lateral-oblique cyclic loading on abutment screw loosening of internal and external hexagon implants," *Dental Materials Journal*, 2009.

[66] E. Weiss, "Effect of repeated closures on opening torque values in seven abutment-implant systems," *The Journal of prosthetic dentistry*, 2000.

[67] J.-G. Wittneben, D. Buser, G. E. Salvi, W. Bürgin, S. Hicklin, and U. Brägger, "Complication and Failure Rates with Implant-Supported Fixed Dental Prostheses and Single Crowns: A 10-Year Retrospective Study," *Clinical implant dentistry and related research*, 2013.

Appendices

A Pilot Study Procedure

1. Turn on Instron 55MT and PC. Open Partner software and open procedure `MCaselliSettlingPilotTest.prc`

2. Select new, unused ST-009-M1.6 (threaded insert)

3. Select new, unused ST-005-02 (hex insert)

4. Place ST-005-02 into the hex-shaped recess of ST-003, and mark the top side of the hex insert, e.g. with a dot of permanent marker. Keep the marking outside of the seating surface of the screw.

5. Measure the combined thickness (l_a) of the hex insert and the lid using height gauge

6. Compute required projection (l_p) of the threaded insert based on the following formula:

$$l_p = C + l_a + l_e - l_s \tag{A.1}$$

   where $C = 15.25\,\text{mm}$, a constant of the fixture, and l_s is the "shank length" of the screw, equal to $l_b + l_t + l_e$.

   For this pilot study, $l_e = 2.4\,\text{mm}$, 1.5 times the nominal diameter of the M1.6 screw, and for SCR-0680 $l_s = 8.35\,\text{mm}$, so (A.1) reduces to:

$$l_p = 9.3\,\text{mm} + l_a \tag{A.2}$$

7. Thread the threaded insert into ST-010 (square boss)

8. Check the projection (distance between the top surface of the square boss and the top surface of the threaded insert, adjacent to the set screw)

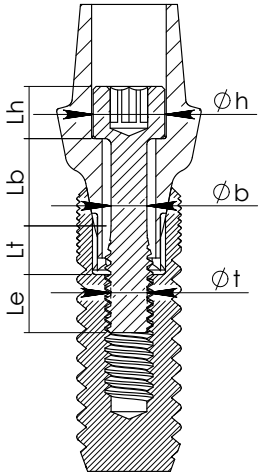

Figure 38: Cross section of an implant-screw-abutment assembly showing critical abutment screw dimensions

using a height gauge. Adjust the projection as necessary to achieve the desired value by turning the threaded insert in the square boss.

9. Tighten the set screw in the square boss to lock the threaded insert in place.

10. Confirm the projection using the height gauge. Projection must be within the range $l_p \pm 0.05\,\text{mm}$

11. Place the load cell into the central recess of ST-012 (housing), with the hollow side of the load cell facing down

12. Insert the threaded insert/square boss assembly up through the bottom of the housing and through the load cell

13. Place the hex insert into the hex-shaped recess in the lid, ensuring that the hex insert is oriented with the "top" mark made earlier facing up

14. Place the lid/hex insert assembly onto the load cell housing assembly, lining up the locating pins on the housing with the corresponding holes on the lid

15. Select new, unused SCR-0680 (abutment screw), and thread by hand through the hex insert and into the threaded insert, until first resistance is felt—Do Not Tighten—then back off ½ turn

16. Insert abutment screw driver in 3-jaw chuck on Instron 55MT power head, tighten securely using chuck key.

17. Slide load cell housing assembly into mating fixture on Instron 55MT tailstock.

18. While holding tailstock, release black locking lever to allow tailstock to slide freely on load frame. Do not allow tailstock to crash into abutment screw driver. Slowly allow tailstock to move towards abutment screw driver.

19. Check alignment of abutment screw driver with abutment screw, both in the vertical direction and the machine-transverse direction. With the abutment screw driver a few millimeters away from the abutment screw, use the keypad to rotate the power head while observing alignment, as there may be some runout of the abutment screw driver in the machine.

20. If the alignment between the screw driver and the abutment screw needs to be adjusted, move the tailstock away from the driver and lock the tailstock in place on the slide using the black lever. If vertical alignment adjustment is needed, loosen the lock nut on the thumbscrew at the bottom of the fixture, and adjust vertical alignment with the thumbscrew. If transverse alignment adjustment is needed, release the red handle to disengage the torsional load cell. Remove the axial load cell assembly to provide access to the retaining bolts for the mating fixture. Loosen mounting bolts to adjust transverse alignment. Re-secure all mounting

bolts and lock nut, replace axial load cell in the fixture, and engage the torsional load cell by tightening the red handle. Check alignment to screw driver and repeat adjustment if necessary.

21. Once alignment of abutment screw driver and abutment screw is satisfactory, while holding tailstock, release black locking lever to allow tailstock to slide freely on load frame. Do not allow tailstock to crash into abutment screw driver. Slowly allow tailstock to move towards abutment screw driver, until the abutment screw is in contact with the abutment screw driver. Engage the abutment screw driver in the drive feature of the abutment screw. Often the screw driver must be rotated to allow engagement. If this is the case, use the keypad to rotate the driver by tapping the button labeled "LOOSEN" repeatedly until engagement is observed.

22. Close safety cover on Instron 55MT

23. Confirm that the active test results database is `MCaselliSettlingPilotTest`

24. Enter required parameter values (Diameter, Pitch, Specimen Identification, Part, Lot, Operator)

25. Initiate the test sequence

26. Ensure signage is posted on and around the test apparatus indicating

    DO NOT DISTURB

    Long-term testing in progress

    Contact M. Caselli

27. Leave the apparatus undisturbed for the duration of the test sequence

28. Upon completion of the test sequence, click the "save result" icon on the partner software toolbar.

29. Press the LOOSEN button repeatedly to loosen the abutment screw, until the on-screen load display reads in the range 0 ± 10 N.

30. Remove the axial load cell assembly from the tailstock. Remove the abutment screw, hex insert, and threaded insert, and package each in an individual bag labeled with the serial number of the test (i.e. the "test counter" from the Instron Partner software).

B Pilot Study Test Program

1. Tighten at 6 RPM to 2 N-cm; Data aquisition at 500 Hz, keep every 50th sample (10 sample/sec)

2. Tighten at 2 N-cm/s to 25 N-cm; Data aquisition at 500 Hz, keep every 50th sample (10 sample/sec)

3. Reduce torque at 25 N-cm/s to 0 N-cm; Data aquisition at 500 Hz, keep every 50th sample (10 sample/sec)

4. Hold angle for 15 min; Data aquisition at 500 Hz, keep every 50th sample (10 sample/sec)

5. Hold angle for 11.75 hr; Data aquisition at 10 Hz, keep every 300th sample (2 sample/min)

Problems with current test program:

- overshoot of target tightening torque (now down to approx. 0.3 N-cm, an acceptable level)

C List of Materials and Apparatus for Main Study

- Qty. 90 ST-005-12 “hex insert” (consumable)
- Qty. 90 ST-005-13 “hex insert” (consumable)
- Qty. 180 ST-009-M1.6 “threaded insert” (consumable)
- Qty. 90 Screw Ref#5979 “flat abutment screw” (consumable)
- Qty. 90 Screw Ref#5764 “tapered abutment screw” (consumable)
- Abutment screw driver, 1.25 mm hex
- ST-003 “lid”
- ST-012 “housing”
- ST-010 “square boss”
- Instron 55MT with donut load cell, (1) 3-jaw chuck, and deadweight setup
- Height gauge
- 1.5 mm hex driver for set screw
- Powderless rubber exam gloves (latex or nitrile)
- Plastic tweezers

D Main Study Procedures

NOTE: Handle abutment screws, hex inserts, and threaded inserts with plastic tweezers, or clean gloved hands only.

1. Consult randomization plan to determine what type of text the next sample should be.

	5979	5764
Hex Insert	ST-005-13	ST-005-12
l_h	1.80 mm	2.09 mm
l_c	0 mm	0.49 mm
l_b	1.56 mm	1.62 mm
l_t	2.04 mm	1.34 mm
l_e	2.40 mm	2.40 mm
l_s	6.00 mm	5.85 mm
$(l_p - l_a)$	11.65 mm	11.80 mm
l_p	11.65 mm + l_a	11.80 mm + l_a

Table 25: Screw dimensions

Protocol	Procedure Filename
T	`MCaselliSettlingTestGroupT.prc`
TT	`MCaselliSettlingTestGroupTT.prc`
TLT	`MCaselliSettlingTestGroupTLT.prc`

Table 26: Instron Partner software test procedures

2. If not already on and running, turn on Instron 55MT and PC. Open Partner software.

3. Open the appropriate test procedure (see Table 26)

4. Select new, unused ST-005 (hex insert). Choose ST-005-12 or ST-005-13 based on the randomization plan and the information in Table 25

5. Place ST-005 into the hex-shaped recess of ST-003. If using ST-005-12 (with countersink), be sure the countersink faces up. If using ST-005-13 (without countersink), mark the top surface of the hex insert with a dot of permanent marker, making sure to keep the mark outside of the region that will contact the screw head.

6. Measure the combined thickness (l_a) of the hex insert and the lid using height gauge. Record the result in notebook alongside the sample number.

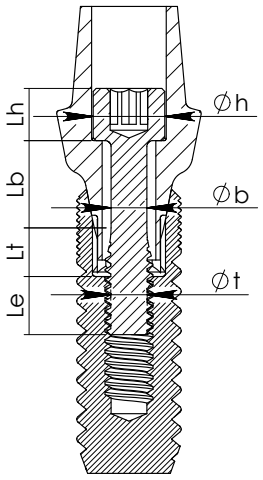

Figure 39: Cross section of an implant-screw-abutment assembly showing critical abutment screw dimensions

7. Compute required projection (l_p) of the threaded insert according to Table 25. Record the result in notebook alongside the sample number.

8. Select new, unused ST-009-M1.6 (threaded insert)

9. Thread the threaded insert into ST-010 (square boss)

10. Check the projection (distance between the top surface of the square boss and the top surface of the threaded insert, adjacent to the set screw) using a height gauge. Adjust the projection as necessary to achieve the desired value by turning the threaded insert in the square boss.

11. Tighten the set screw in the square boss to lock the threaded insert in place.

12. Confirm the projection using the height gauge. Projection must be within the range $l_p \pm 0.05\,\text{mm}$. Record the actual projection in notebook alongside sample number.

13. Place the load cell into the central recess of ST-012 (housing), with the hollow side of the load cell facing down

14. Insert the threaded insert/square boss assembly up through the bottom of the housing and through the load cell

15. Place the hex insert into the hex-shaped recess in the lid, ensuring that the hex insert is oriented with the "top" mark made earlier facing up

16. Place the lid/hex insert assembly onto the load cell housing assembly, lining up the locating pins on the housing with the corresponding holes on the lid

17. Select new, unused abutment screw, according to the randomization plan, and thread by hand through the hex insert and into the threaded insert, until first resistance is felt—Do Not Tighten—then back off $1/2$ turn

18. Insert abutment screw driver in 3-jaw chuck on Instron 55MT power head, tighten securely using chuck key.

19. Slide load cell housing assembly into mating fixture on Instron 55MT tailstock.

20. While holding tailstock, release black locking lever to allow tailstock to slide freely on load frame. Do not allow tailstock to crash into abutment screw driver. Slowly allow tailstock to move towards abutment screw driver.

21. Check alignment of abutment screw driver with abutment screw, both in the vertical direction and the machine-transverse direction. With the abutment screw driver a few millimeters away from the abutment screw, use the keypad to rotate the power head while observing alignment, as there may be some runout of the abutment screw driver in the machine.

22. If the alignment between the screw driver and the abutment screw needs to be adjusted, move the tailstock away from the driver and lock the tailstock in place on the slide using the black lever. If vertical alignment adjustment is needed, loosen the lock nut on the thumbscrew at the bottom of the fixture, and adjust vertical alignment with the thumbscrew. If transverse alignment adjustment is needed, release the red handle to disengage the torsional load cell. Remove the axial load cell assembly to provide access to the retaining bolts for the mating fixture. Loosen mounting bolts to adjust transverse alignment. Re-secure all mounting bolts and lock nut, replace axial load cell in the fixture, and engage the torsional load cell by tightening the red handle. Check alignment to screw driver and repeat adjustment if necessary.

23. Once alignment of abutment screw driver and abutment screw is satisfactory, while holding tailstock, release black locking lever to allow tailstock to slide freely on load frame. Do not allow tailstock to crash into abutment screw driver. Slowly allow tailstock to move towards abutment screw driver, until the abutment screw is in contact with the abutment screw driver. Engage the abutment screw driver in the drive feature of the abutment screw. Often the screw driver must be rotated to allow engagement. If this is the case, use the keypad to rotate the driver by tapping the button labeled "LOOSEN" repeatedly until engagement is observed.

24. Close safety cover on Instron 55MT

25. Enter required parameter values: Diameter, Pitch, Specimen Identification (use sample number from randomization plan), Part, Lot, Operator

26. Confirm that the active test results database is `MCaselliThesis`

27. Confirm that the active procedure is appropriate for the protocol according to the randomization plan (see Table 26).

28. Initiate the test sequence

29. If conducting a 2 hour test, set a timer or alarm for 2 hours.

30. Ensure signage is posted on and around the test apparatus indicating

    DO NOT DISTURB
    Long-term testing in progress
    Contact M. Caselli

31. Leave the apparatus undisturbed for the duration of the test sequence (2 hours or 12 hours, as per the randomization plan).

32. If conducting a 2 hour test, at the conclusion of the 2 hour observation period, click the "stop test" icon on the Partner software toolbar.

33. Upon completion of the test sequence, click the "save result" icon on the partner software toolbar.

34. Press the LOOSEN button repeatedly to loosen the abutment screw, until the on-screen load display reads in the range 0 ± 10 N.

35. Remove the axial load cell assembly from the tailstock. Remove the abutment screw, hex insert, and threaded insert, and package each in an individual bag labeled with the Sample ID from the randomization plan and the serial number of the test (i.e. the "test counter" from the Instron Partner software).

36. Save a copy of the results database daily to a removable drive. Version the file by appending a datestamp to the filename.

E Tabular Data: 2 Hours

Table 27: Raw data, observations after 2 hours, flat screw

Specimen ID	Protocol	Peak Torque (N-cm)	P_1 (N)	P_2 (N)	Residual Preload (N)	Preload Loss (N)	Relative Preload Loss
2.S3	T	25.2	382		376	6	1.6%
2.S11	T	25.4	397		389	7	1.9%
12.S6	T	25.3	369		361	7	1.9%
2.S16	T	25.2	376		366	10	2.7%
2.S23	T	25.4	395		387	8	2.0%
2.S26	T	25.3	388		378	10	2.5%
12.S9	T	25.3	386		378	8	2.0%
2.S31	T	25.4	407		402	6	1.4%
2.S39	T	25.3	390		383	7	1.9%
12.S14	T	25.1	392		386	7	1.7%
2.S47	T	25.1	386		378	8	2.1%
2.S52	T	25.4	391		385	6	1.6%
2.S60	T	25.2	388		381	7	1.7%
12.S23	T	25.3	378		372	6	1.5%
2.S65	T	25.3	368		361	7	2.0%
12.S25	T	25.3	376		370	6	1.5%
2.S68	T	25.1	358		354	4	1.2%
2.S76	T	25.3	378		372	6	1.6%
12.S31	T	25.3	373		367	6	1.6%
2.S82	T	25.4	389		382	6	1.7%
2.S90	T	25.4	366		353	12	3.4%
2.S95	T	25.3	340		325	15	4.3%
12.S37	T	25.3	377		365	13	3.3%
2.S1	TT	25.3	378	370	367	3	0.8%
12.S2	TT	25.3	393	388	385	3	0.7%
2.S10	TT	25.3	385	376	373	3	0.7%
2.S18	TT	25.2	390	384	381	3	0.7%
2.S19	TT	25.1	379	374	371	3	0.9%
12.S8	TT	25.3	384	375	372	3	0.8%
2.S28	TT	25.4	375	365	362	3	0.9%
2.S36	TT	25.3	375	372	369	3	0.7%
2.S38	TT	25.1	373	369	366	3	0.8%
2.S44	TT	25.3	399	396	394	2	0.5%
12.S16	TT	25.1	380	372	369	3	0.8%
2.S49	TT	25.3	383	377	374	3	0.8%
2.S56	TT	25.4	390	387	385	2	0.4%
12.S20	TT	25.4	386	381	378	3	0.7%

Table 27: Raw data, observations after 2 hours, flat screw

Specimen ID	Protocol	Peak Torque (N-cm)	P_1 (N)	P_2 (N)	Residual Preload (N)	Preload Loss (N)	Relative Preload Loss
2.S63	TT	25.3	388	383	380	3	0.7%
2.S70	TT	25.1	376	373	370	3	0.8%
12.S28	TT	25.3	416	411	409	2	0.5%
2.S75	TT	25.3	400	397	394	3	0.6%
12.S32	TT	25.1	358	354	351	2	0.6%
2.S84	TT	25.2	355	346	343	3	1.0%
2.S89	TT	25.3	379	368	364	4	1.2%
2.S93	TT	25.3	368	361	357	3	1.0%
12.S40	TT	25.3	400	388	385	3	0.9%
2.S99	TT	25.1	393	383	379	4	1.0%
2.S7	TLT	25.2	373	364	360	4	1.0%
12.S4	TLT	25.4	384	372	369	4	1.0%
2.S17	TLT	25.4	389	372	367	5	1.3%
2.S21	TLT	25.2	390	379	375	5	1.2%
2.S25	TLT	25.4	405	377	371	5	1.4%
2.S34	TLT	25.4	360	375	371	5	1.3%
12.S11	TLT	25.3	381	370	365	5	1.5%
2.S42	TLT	25.4	382	366	359	7	1.9%
2.S46	TLT	25.5	359	377	372	5	1.4%
12.S17	TLT	25.4	371	364	360	5	1.3%
2.S54	TLT	25.5	384	392	386	6	1.4%
2.S55	TLT	25.5	377	365	361	4	1.0%
2.S61	TLT	25.3	389	374	371	3	0.8%
12.S24	TLT	25.4	391	371	367	4	1.1%
12.S26	TLT	25.2	360	362	358	4	1.1%
2.S69	TLT	25.4	391	382	378	4	1.0%
2.S78	TLT	25.2	360	376	370	6	1.5%
2.S83	TLT	25.3	397	376	372	4	1.0%
12.S33	TLT	25.3	367	364	356	9	2.3%
2.S87	TLT	25.4	388	386	379	7	1.8%
2.S92	TLT	25.3	384	362	356	6	1.7%
12.S39	TLT	25.3	392	373	367	6	1.6%
2.S100	TLT	25.3	367	369	358	11	2.9%

Table 28: Raw data, observations after 2 hours, tapered screw

Specimen ID	Protocol	Peak Torque (N-cm)	P_1 (N)	P_2 (N)	Residual Preload (N)	Preload Loss (N)	Relative Preload Loss
12.S1	T	25.3	225		218	6	2.9%
2.S6	T	25.1	237		229	7	3.2%
2.S12	T	25.4	236		228	8	3.5%
2.S15	T	25.4	240		229	10	4.3%
12.S7	T	25.1	247		240	7	2.8%
2.S24	T	25.1	240		232	8	3.2%
2.S29	T	25.2	236		229	6	2.8%
2.S35	T	25.3	230		222	7	3.3%
2.S40	T	25.2	226		214	12	5.2%
2.S45	T	25.3	231		220	11	4.8%
2.S51	T	25.2	218		213	5	2.3%
12.S18	T	25.2	245		241	4	1.8%
2.S57	T	25.3	239		228	11	4.6%
12.S21	T	25.2	234		226	9	3.7%
2.S62	T	25.2	256		251	5	2.0%
2.S72	T	25.1	245		241	3	1.4%
2.S74	T	25.4	246		239	8	3.1%
12.S29	T	25.4	247		239	8	3.0%
2.S80	T	25.3	223		207	16	7.1%
2.S85	T	25.4	224		215	8	3.6%
2.S91	T	25.1	250		239	11	4.3%
2.S98	T	25.3	229		222	7	3.2%
12.S41	T	25.4	233		228	4	1.9%
2.S4	TT	25.1	223	225	221	4	1.8%
12.S3	TT	25.3	228	230	226	4	1.7%
2.S9	TT	25.1	242	236	235	2	0.7%
2.S14	TT	25.3	248	243	241	2	0.7%
2.S22	TT	25.2	229	226	224	2	0.9%
2.S27	TT	25.3	242	239	236	3	1.1%
2.S33	TT	25.2	231	232	228	3	1.4%
12.S12	TT	25.4	238	230	228	2	1.0%
2.S41	TT	25.3	236	233	230	3	1.3%
2.S43	TT	25.2	228	231	228	3	1.1%
12.15	TT	25.2	237	232	231	2	0.7%
2.S53	TT	25.2	248	243	241	2	0.8%
2.S58	TT	25.2	230	231	229	3	1.2%
21.S22	TT	25.4	242	236	234	3	1.1%
2.S66	TT	25.3	243	239	235	4	1.6%
2.S71	TT	25.1	213	218	214	3	1.5%
2.S77	TT	25.3	224	221	219	2	0.8%

Table 28: Raw data, observations after 2 hours, tapered screw

Specimen ID	Protocol	Peak Torque (N-cm)	P_1 (N)	P_2 (N)	Residual Preload (N)	Preload Loss (N)	Relative Preload Loss
2.S79	TT	25.1	236	234	233	1	0.5%
12.S30	TT	25.4	237	241	240	1	0.6%
2.S86	TT	25.3	237	234	232	2	0.7%
12.S35	TT	25.2	239	234	232	2	0.8%
2.S96	TT	25.1	249	244	242	2	0.9%
2.S101	TT	25.3	226	229	226	3	1.2%
2.S5	TLT	25.3	226	233	230	4	1.5%
2.S8	TLT	25.3	239	246	241	5	1.9%
12.S5	TLT	25.4	225	231	224	7	2.8%
2.S13	TLT	25.3	239	243	238	5	2.2%
2.S20	TLT	25.3	229	234	229	5	2.2%
2.S30	TLT	25.2	215	233	227	6	2.4%
12.S10	TLT	25.4	231	237	232	5	2.1%
2.S32	TLT	25.2	228	241	236	5	2.1%
2.S37	TLT	25.4	245	247	243	5	1.9%
12.S13	TLT	25.4	240	248	243	5	1.9%
2.S48	TLT	25.2	240	250	246	4	1.6%
2.S50	TLT	25.4	234	254	252	3	1.1%
12.S19	TLT	25.3	247	246	244	3	1.2%
2.S59	TLT	25.4	225	242	237	5	2.1%
2.S64	TLT	25.1	248	241	237	4	1.6%
2.S67	TLT	25.3	231	244	241	3	1.4%
12.S27	TLT	25.3	224	237	235	2	0.9%
2.S81	TLT	25.4	239	247	242	5	1.9%
12.S34	TLT	25.4	228	235	231	4	1.8%
2.S88	TLT	25.3	266	255	252	3	1.1%
2.S94	TLT	25.4	242	244	241	3	1.2%
12.S38	TLT	25.3	220	231	228	3	1.4%
2.S97	TLT	25.3	235	243	238	5	2.1%

F Tabular Data: 12 Hours

Table 29: Raw data, observations after 12 hours, flat screw

Specimen ID	Protocol	Peak Torque (N-cm)	P_1 (N)	P_2 (N)	Residual Preload (N)	Preload Loss (N)	Relative Preload Loss
12.S6	T	25.3	369		360	8	2.2%
2.S26	T	25.3	388		377	11	2.8%
12.S9	T	25.3	386		377	9	2.3%
12.S14	T	25.1	392		384	8	2.1%
12.S23	T	25.3	378		371	7	1.8%
12.S25	T	25.3	376		370	7	1.8%
12.S31	T	25.3	373		366	7	1.8%
12.S37	T	25.3	377		363	14	3.6%
12.S2	TT	25.3	393	388	385	4	0.9%
12.S8	TT	25.3	384	375	370	5	1.2%
12.S16	TT	25.1	380	372	368	4	1.1%
12.S20	TT	25.4	386	381	377	4	1.0%
12.S28	TT	25.3	416	411	408	3	0.7%
12.S32	TT	25.1	358	354	350	3	0.9%
12.S40	TT	25.3	400	388	383	5	1.3%
12.S4	TLT	25.4	384	372	368	5	1.2%
2.S21	TLT	25.2	390	379	373	6	1.6%
12.S11	TLT	25.3	381	370	364	6	1.8%
12.S17	TLT	25.4	371	364	359	6	1.6%
12.S24	TLT	25.4	391	371	366	5	1.3%
12.S26	TLT	25.2	360	362	357	5	1.4%
12.S33	TLT	25.3	367	364	355	9	2.6%
12.S39	TLT	25.3	392	373	366	7	2.0%

Table 30: Raw data, observations after 12 hours, tapered screw

Specimen ID	Protocol	Peak Torque (N-cm)	P_1 (N)	P_2 (N)	Residual Preload (N)	Preload Loss (N)	Relative Preload Loss
12.S1	T	25.3	225		218	7	3.0%
12.S7	T	25.1	247		239	8	3.1%
12.S18	T	25.2	245		240	5	1.9%
12.S21	T	25.2	234		225	9	4.0%
12.S29	T	25.4	247		239	8	3.2%
12.S41	T	25.4	233		228	5	2.2%
12.S3	TT	25.3	228	230	225	4	1.9%
12.S12	TT	25.4	238	230	227	3	1.4%
12.15	TT	25.2	237	232	230	3	1.2%
21.S22	TT	25.4	242	236	233	3	1.2%

Table 30: Raw data, observations after 12 hours, tapered screw

Specimen ID	Protocol	Peak Torque (N-cm)	P_1 (N)	P_2 (N)	Residual Preload (N)	Preload Loss (N)	Relative Preload Loss
12.S30	TT	25.4	237	241	239	2	0.8%
12.S35	TT	25.2	239	234	232	2	1.1%
12.S5	TLT	25.4	225	231	223	8	3.3%
12.S10	TLT	25.4	231	237	231	6	2.3%
12.S13	TLT	25.4	240	248	242	6	2.3%
12.S19	TLT	25.3	247	246	243	4	1.6%
12.S34	TLT	25.4	228	235	230	5	2.3%
12.S38	TLT	25.3	220	231	227	4	1.8%

G Randomization Plan

Table 31: Randomization plan for 2-hour observation period

Sample ID	Block	Screw	Protocol
2.S1	1	5979	TT
2.S2	1	5979	TLT
2.S3	1	5979	T
2.S4	1	5764	TT
2.S5	1	5764	TLT
2.S6	1	5764	T
2.S7	2	5979	TLT
2.S8	2	5764	TLT
2.S9	2	5764	TT
2.S10	2	5979	TT
2.S11	2	5979	T
2.S12	2	5764	T
2.S13	3	5764	TLT
2.S14	3	5764	TT
2.S15	3	5764	T
2.S16	3	5979	T
2.S17	3	5979	TLT
2.S18	3	5979	TT
2.S19	4	5979	TT
2.S20	4	5764	TLT
2.S21	4	5979	TLT
2.S22	4	5764	TT
2.S23	4	5979	T

Table 31: Randomization plan for 2-hour observation period

Sample ID	Block	Screw	Protocol
2.S24	4	5764	T
2.S25	5	5979	TLT
2.S26	5	5979	T
2.S27	5	5764	TT
2.S28	5	5979	TT
2.S29	5	5764	T
2.S30	5	5764	TLT
2.S31	6	5979	T
2.S32	6	5764	TLT
2.S33	6	5764	TT
2.S34	6	5979	TLT
2.S35	6	5764	T
2.S36	6	5979	TT
2.S37	7	5764	TLT
2.S38	7	5979	TT
2.S39	7	5979	T
2.S40	7	5764	T
2.S41	7	5764	TT
2.S42	7	5979	TLT
2.S43	8	5764	TT
2.S44	8	5979	TT
2.S45	8	5764	T
2.S46	8	5979	TLT
2.S47	8	5979	T
2.S48	8	5764	TLT
2.S49	9	5979	TT
2.S50	9	5764	TLT
2.S51	9	5764	T
2.S52	9	5979	T
2.S53	9	5764	TT
2.S54	9	5979	TLT
2.S55	10	5979	TLT
2.S56	10	5979	TT
2.S57	10	5764	T
2.S58	10	5764	TT
2.S59	10	5764	TLT
2.S60	10	5979	T
2.S61	11	5979	TLT
2.S62	11	5764	T
2.S63	11	5979	TT
2.S64	11	5764	TLT
2.S65	11	5979	T

Table 31: Randomization plan for 2-hour observation period

Sample ID	Block	Screw	Protocol
2.S66	11	5764	TT
2.S67	12	5764	TLT
2.S68	12	5979	T
2.S69	12	5979	TLT
2.S70	12	5979	TT
2.S71	12	5764	TT
2.S72	12	5764	T
2.S73	13	5764	TLT
2.S74	13	5764	T
2.S75	13	5979	TT
2.S76	13	5979	T
2.S77	13	5764	TT
2.S78	13	5979	TLT
2.S79	14	5764	TT
2.S80	14	5764	T
2.S81	14	5764	TLT
2.S82	14	5979	T
2.S83	14	5979	TLT
2.S84	14	5979	TT
2.S85	15	5764	T
2.S86	15	5764	TT
2.S87	15	5979	TLT
2.S88	15	5764	TLT
2.S89	15	5979	TT
2.S90	15	5979	T
2.S91	16	5764	T
2.S92	16	5979	TLT
2.S93	16	5979	TT
2.S94	16	5764	TLT
2.S95	16	5979	T
2.S96	16	5764	TT
2.S97	17	5764	TLT
2.S98	17	5764	T
2.S99	17	5979	TT
2.S100	17	5979	TLT
2.S101	17	5764	TT
2.S102	17	5979	T
2.S103	18	5764	TT
2.S104	18	5764	TLT
2.S105	18	5979	TT
2.S106	18	5979	T
2.S107	18	5979	TLT

Table 31: Randomization plan for 2-hour observation period

Sample ID	Block	Screw	Protocol
2.S108	18	5764	T
2.S109	19	5764	TT
2.S110	19	5764	T
2.S111	19	5979	TLT
2.S112	19	5764	TLT
2.S113	19	5979	T
2.S114	19	5979	TT
2.S115	20	5764	TLT
2.S116	20	5764	T
2.S117	20	5764	TT
2.S118	20	5979	TLT
2.S119	20	5979	TT
2.S120	20	5979	T
2.S121	21	5979	TLT
2.S122	21	5979	TT
2.S123	21	5764	TLT
2.S124	21	5764	T
2.S125	21	5764	TT
2.S126	21	5979	T
2.S127	22	5764	T
2.S128	22	5979	T
2.S129	22	5764	TLT
2.S130	22	5764	TT
2.S131	22	5979	TT
2.S132	22	5979	TLT
2.S133	23	5764	TLT
2.S134	23	5979	TLT
2.S135	23	5764	TT
2.S136	23	5979	TT
2.S137	23	5979	T
2.S138	23	5764	T

Table 32: Randomization plan for 12-hour observation period

Sample ID	Block	Screw	Protocol
12.S1	1	5764	T
12.S2	1	5979	TT
12.S3	1	5764	TT
12.S4	1	5979	TLT
12.S5	1	5764	TLT
12.S6	1	5979	T
12.S7	2	5764	T
12.S8	2	5979	TT
12.S9	2	5979	T
12.S10	2	5764	TLT
12.S11	2	5979	TLT
12.S12	2	5764	TT
12.S13	3	5764	TLT
12.S14	3	5979	T
12.S15	3	5764	TT
12.S16	3	5979	TT
12.S17	3	5979	TLT
12.S18	3	5764	T
12.S19	4	5764	TLT
12.S20	4	5979	TT
12.S21	4	5764	T
12.S22	4	5764	TT
12.S23	4	5979	T
12.S24	4	5979	TLT
12.S25	5	5979	T
12.S26	5	5979	TLT
12.S27	5	5764	TLT
12.S28	5	5979	TT
12.S29	5	5764	T
12.S30	5	5764	TT
12.S31	6	5979	T
12.S32	6	5979	TT
12.S33	6	5979	TLT
12.S34	6	5764	TLT
12.S35	6	5764	TT
12.S36	6	5764	T
12.S37	7	5979	T
12.S38	7	5764	TLT
12.S39	7	5979	TLT
12.S40	7	5979	TT
12.S41	7	5764	T
12.S42	7	5764	TT

H Randomization Plan for Roughness Measurement

Table 33: Randomization Plan for Roughness Evaluation

Block	Protocol	Test Counter	Sample ID
1	TLT	2835	2.S83
1	unused	N/A	N/A
1	TT	2735	2.S10
1	T	2742	12.S6
2	TT	2747	2.S19
2	T	2807	12.S23
2	TLT	2828	2.S78
2	unused	N/A	N/A
3	TLT	2839	12.S33
3	unused	N/A	N/A
3	T	2801	2.S60
3	TT	2817	2.S70
4	TLT	2776	2.S42
4	T	2846	2.S90
4	unused	N/A	N/A
4	TT	2722	2.S1
5	TT	2779	2.S44
5	unused	N/A	N/A
5	T	2814	2.S68
5	TLT	2788	12.S17
6	TT	2752	12.S8
6	T	2790	2.S52
6	unused	N/A	N/A
6	TLT	2815	12.S26
7	TLT	2861	2.S100
7	TT	2785	12.S16
7	unused	N/A	N/A
7	T	2725	2.S3
8	T	2743	2.S16
8	TT	2798	12.S20
8	TLT	2765	2.S34
8	unused	N/A	N/A
9	T	2777	12.S14
9	TLT	2734	12.S4
9	unused	N/A	N/A
9	TT	2757	2.S28

Table 33: Randomization Plan for Roughness Evaluation

Block	Protocol	Test Counter	Sample ID
10	unused	N/A	N/A
10	TLT	2848	2.S92
10	TT	2824	2.S75
10	T	2761	2.S31